# Characterization of the coastal marine environment in the vicinity of a grounded iceberg, Canadian Arctic Archipelago

by

Melissa Nacke

A thesis submitted to the Faculty of Graduate and Postdoctoral Affairs in partial fulfillment of the requirements for the degree of

Master of Science

in

Geography

Carleton University
Ottawa, Ontario

## Abstract

This study aimed to characterize the marine environment in the vicinity of a grounded iceberg near Resolute, Nunavut, and evaluate its potential influence on the surrounding water column. A survey of the physico-chemical properties (salinity, temperature and $\delta^{18}O$, as well as nitrate, phosphate and silicic acid concentrations) and phytoplankton biomass was conducted from August 11$^{th}$ to 29$^{th}$, 2014. The water column was strongly stratified throughout the study area due to sea ice melt. The iceberg's interference with the ocean currents resulted in mixing and potentially upwelling in the adjacent water column. A phytoplankton bloom, indicated by high chlorophyll *a* concentrations (13.7 to 21.0 mg $m^{-3}$) and surface nutrient depletion, was observed and likely began prior to sea ice break up on August 9$^{th}$. The presence of icebergs on Arctic continental shelves may influence local coastal current dynamics, although it did not appear to influence nutrient dynamics during this study.

## Acknowledgements

This thesis could not have been realized without a great deal of guidance and support. I would like to thank my supervisor, Dr. Derek Mueller, who patiently encouraged me throughout my thesis and contributed his knowledge to the project whilst allowing me the room to also work independently. I would also like to thank my co-supervisor, Dr. Christine Michel, whose enthusiasm and charisma provided a positive and motivated learning environment. Over the past two years I have benefited greatly from Derek and Christine's constructive criticism, comments, and suggestions.

My fieldwork in Resolute, Nunavut could not have been accomplished without my field assistant, Sam Brenner, as well as my local guides, Ross Pudluk, and Peter and Jeffery Amaruliq. These individuals demonstrated a great deal of dedication to my research project and tolerated my obsessive tendencies regarding the fieldwork. I would like to thank Ross for satisfying my curiosity by answering my many Qallunaat questions.

During my time at Carleton University I was surrounded by a friendly and cheerful group of fellow students and colleagues. I would like to acknowledge the Department of Geography and Environmental Studies and the Water and Ice Research Laboratory, as well as the Freshwater Institute (Fisheries and Oceans Canada). In particular, I greatly appreciate Murray Richardson, Andrea Niemi, Claude Belzile, and Sarah Zimmermann for help with the field preparation and/or sample processing. I would also like to thank Andrew Hamilton for taking the time to provide advice on data analysis.

This research was made possible by the financial and technical support of numerous organizations. This includes the Natural Sciences and Engineering Research Council of Canada, Northern Scientific Training Program, ArcticNet, the Canadian Foundation for Innovation, the Ontario Ministry of Innovation, the Ontario Research Fund, the Polar Continental Shelf Program, Fisheries and Oceans Canada, First Air and the Arctic Circle.

Lastly, I would like to thank my friends and family for maintaining my sanity and providing unconditional support in every endeavour I take on.

**Table of Contents**

## List of Figures

## List of Tables

# List of Appendices

# 1 Chapter: Introduction

The Arctic cryosphere has undergone dramatic changes in the past few decades, with warming in the Arctic being approximately two times greater than the global average (Cohen et al. 2014). A feedback response between ice cover and albedo suggests that this warming and the associated retreat of ice cover in the Arctic will only increase in the future (Serreze and Barry 2011). A consequence of rapid warming in the Arctic is an increase in calving events of ice shelves (Mueller et al. 2003) and floating glacier tongues (Rignot and Steffen 2008), which create expansive tabular icebergs known as ice islands (Peterson 2005). Similarly, there is evidence that the frequency of iceberg calving events from Antarctica ice shelves is also increasing (Long et al. 2002). These ice islands can deteriorate into multiple pieces, producing irregularly shaped icebergs. There is evidence that free-drifting icebergs in the Antarctic could be surrounded by an abundance of different species at all trophic levels and due to their influence on the surrounding water column can possibly be classified as 'hotspots' of biological enrichment (Smith et al. 2007; Schwarz and Schodlok 2009). Previous literature indicates that this increase in biological activity, often assessed by increased phytoplankton abundance and primary productivity, is caused by an increase in limiting nutrients in the photic zone, which subsequently stimulates growth (Vernet et al. 2011). There are two possible sources of this limiting nutrient: the upwelling of nutrient-rich deep marine waters adjacent to the iceberg (Horne 1985; Stephenson et al. 2011) and the iceberg's own meltwater (Smith et al. 2007).

Melting icebergs can cause density anomalies and changes to the physical structure of the adjacent water column (Stephenson et al. 2011), which can potentially

increase nutrients in the photic zone. Upwelling adjacent to the iceberg can occur as the result of a buoyant convection cell (Kubat et al. 2005; Savage 2001). A buoyant convection cell causes the seawater diluted by the iceberg meltwater to experience a positive buoyancy along the side of the iceberg, causing the adjacent seawater to also rise (Savage 2001; Kubat et al. 2005). Once the rising water reaches an equal density to that of the far-field water it commences to move horizontally, forming a series of stratified layers (Stephenson et al. 2011). Additionally, the iceberg meltwater can form a thin lens of freshwater on the surface, known as a meltwater plume (Donaldson 1978; Helly et al. 2011; Huppert and Turner 1980). Adjacent to the inner boundary layer of rising meltwater is an outer boundary layer of downwelling water, formed due to cabbelling (Garrett and Horne 1978). Cabbelling results when two bodies of water with equal densities but different temperature and salinity combine to have a higher density (Garrett and Horne 1978). Lastly, the presence of an iceberg can alter the structure of the water column by interfering with water currents, resulting in the formation of eddies (Hamner and Hauri 1981), which can cause mixing and upwelling. Any of these density anomalies could allow limiting nutrients to be replenished above the seasonal pycnocline (a location in a water column where density changes rapidly with depth) (Stephenson et al. 2011), thus stimulating biological activity.

Most studies concerning the impacts of icebergs on the surrounding water column have been conducted in the Antarctic (e.g., Arrigo et al. 2002; Cefarelli et al. 2011; Donaldson 1978; Stephenson et al. 2011). There exists only a few studies in the Arctic (e.g., Horne 1985; Stern et al. 2015), none of which are concerned with the influence of icebergs on biological activity. Similar to Antarctic icebergs, it is possible that a

meltwater plume, upwelling due to a buoyant convection cell, as well as downwelling due to cabbelling could also occur near icebergs in the Arctic. It has been suggested that the upwelling associated with a buoyant convection cell could also stimulate phytoplankton growth in the Arctic (Stephenson et al. 2011).

In the Arctic, primary production is constrained by the strong seasonality in light (e.g., Apollonio and Matrai 2011; Gosselin and Legendre 1985) and ice cover (Fortier et al. 2002). The break-up of sea ice and increased light in the late-summer provide favourable conditions for the development of a phytoplankton bloom (Wassmann and Reigstad 2011). During this time, sea ice meltwater is the primary cause of water column stratification (Behrenfeld et al. 2006; Carmack and Wassmann 2006; Carmack 2007; Yamamoto-Kawai et al. 2009), which can be identified by the presence of a strong pycnocline. The strong pycnocline, which acts as a barrier preventing nutrient transportation into the photic zone, also plays an important role in limiting primary production in the Arctic (Tremblay et al. 2011).

Very few studies concerning the impacts of Arctic icebergs on the marine environment have been conducted. This study aims to help fill that knowledge gap and possibly to uncover a 'hotspot' of biological enrichment surrounding Arctic icebergs, similar to those observed in the Antarctic. Therefore, if the results of this study indicate that icebergs are associated with an increase in biological activity, there could be substantial implications concerning local carbon budgets and potentially, the biogeochemistry of Arctic continental shelves.

## 1.1 Research objectives

This study aims to characterize the physical, chemical and biological oceanographic conditions in the vicinity of a grounded iceberg on a Canadian Arctic continental shelf and evaluate its potential influence on the surrounding marine environment. The main objectives were to:

1. Determine the contribution and extent of the iceberg meltwater and its influence on water column structure.
2. Evaluate the influence of an iceberg on phytoplankton biomass and nutrient dynamics.

The research hypotheses, related to these objectives that were addressed are as follows:

1. The fraction of iceberg meltwater will be higher in the upper water column compared to the lower water column.
2. The fraction of iceberg meltwater will be higher at stations directly adjacent to the iceberg compared to all other stations.
3. The main pycnocline will be deeper directly adjacent to the iceberg compared to all other stations.
4. Phytoplankton biomass and nutrient concentrations will be higher at stations directly adjacent to the iceberg compared to all other stations.

## 1.2 Approach

The field program took place near the community of Resolute, Nunavut from August 11$^{th}$ to 29$^{th}$, 2014, where the iceberg under study was grounded. The location of this iceberg provided an unparalleled opportunity to gather multiple samples surrounding an iceberg in the Canadian Arctic Archipelago (CAA). A mixing model was used to

determine the fraction of iceberg and sea ice meltwater in each water sample. Temperature and salinity profiles were used to determine the position of the pycnocline and to characterize the structure of the water column along transects extending away from the iceberg. In order to determine the impacts of the iceberg on the chemical and biological environment, chlorophyll *a* (chl *a*), protist cell abundance and nutrient concentrations were measured adjacent to the iceberg as well as away from the iceberg's area of influence.

### 1.3 Thesis structure

This thesis follows a traditional thesis format. A review of the relevant literature pertaining to the Arctic Ocean, the melting of icebergs and ice islands as well as a limited review of phytoplankton dynamics is presented in Chapter 2. Chapter 3 describes the study site and the methods used to address the above hypotheses. Chapter 4 provides the results of the thesis and Chapter 5 discusses their significance, compares them to other studies and examines some of the limitations of this work. A final chapter (Chapter 6) provides main conclusions and suggests future directions for this topic of research.

# 2 Chapter: Literature review

## 2.1 Arctic physical oceanography

The Arctic Ocean is in exchange with both Pacific and Atlantic Ocean water. Pacific water enters through the narrow and shallow (50 m) Bering Strait while Atlantic water enters through the Fram Strait and the Barents Sea (Rudels et al. 1991, Williams and Carmack, 2015). The Fram Strait has a sill of 2600 m and is the only deep passage into the Arctic Ocean (Rudels et al. 1991). The upper water column in the Arctic Ocean is characterized by a low salinity Surface Mixed Layer (SML). The thickness and the salinity of the SML vary from region to region, while the temperature is at or near the freezing point (Anderson et al. 1994). The low salinity is due in part to continental runoff, primarily via the Siberian rivers, and is controlled by seasonal melting and the freezing of sea ice (Aagaard et al. 1981; Anderson et al. 2013). A pronounced pycnocline, which typically occurs between 50 and 200 m (Aagaard et al. 1981), separates the SML from the warmer Atlantic water (Anderson et al. 2013; Carmack and Wassmann 2006; Carmack 2007; Rudels et al. 1996), thereby reducing the heat flux to the surface ice cover and atmosphere (Aagaard et al. 1981).

The Arctic outflow continental shelves include the CAA (Figure 2.1) and the East Greenland Shelf (Carmack and Wassmann 2006). The outflow shelves are influenced by the physical and biogeochemical changes that take place in the Arctic, such as freezing and melting processes, and river run-off (Carmack and Wassmann 2006; Carmack 2007; Michel et al. 2015; Rudels et al. 1991).

## 2.2 Ice shelves, ice islands and icebergs

Calving of ice shelves (Mueller et al. 2013; Mueller et al. 2008; Peterson 2005) and floating glacier tongues (Rignot and Steffen 2008) creates expansive tabular icebergs known as ice islands (Peterson 2005). The focus of this study is on an iceberg that was likely a fragment of ice island PIIB-Ba which originated from the floating tongue of the Petermann Glacier in northwest Greenland in August 2010 (Luc Desjardins, pers. comm). Ice islands protrude 5 m or more above sea level and can have surface areas ranging between a few thousand square metres to hundreds of square kilometres (WMO 1970). Ice islands are tabular, which implies that they have an extensive horizontal surface, nearly vertical sides and a relatively flat bottom. In contrast, icebergs are irregular in shape (Ballicater Consuting Ltd. 2012) and have a much shorter waterlines compared to ice islands, but relatively large drafts (the maximum depth measurement of the keel or underwater portion of an iceberg).

Ice islands originate from ice shelves and floating glacier tongues (Rudkin et al. 2005). In the Canadian Arctic, ice islands originating from the northern Ellesmere Island ice shelves typically get entrained in the Beaufort Gyre (Jeffries et al. 1987). These ice islands are distinguished by having a ridge and trough surface morphology, which is a characteristic of their parent ice shelves (Jeffries et al. 1987). Ice islands originating from the floating glacier tongues of northwest Greenland commonly drift south through Baffin Bay (Krajick 2001) and continue to drift in the Labrador Current (Newell 1993).

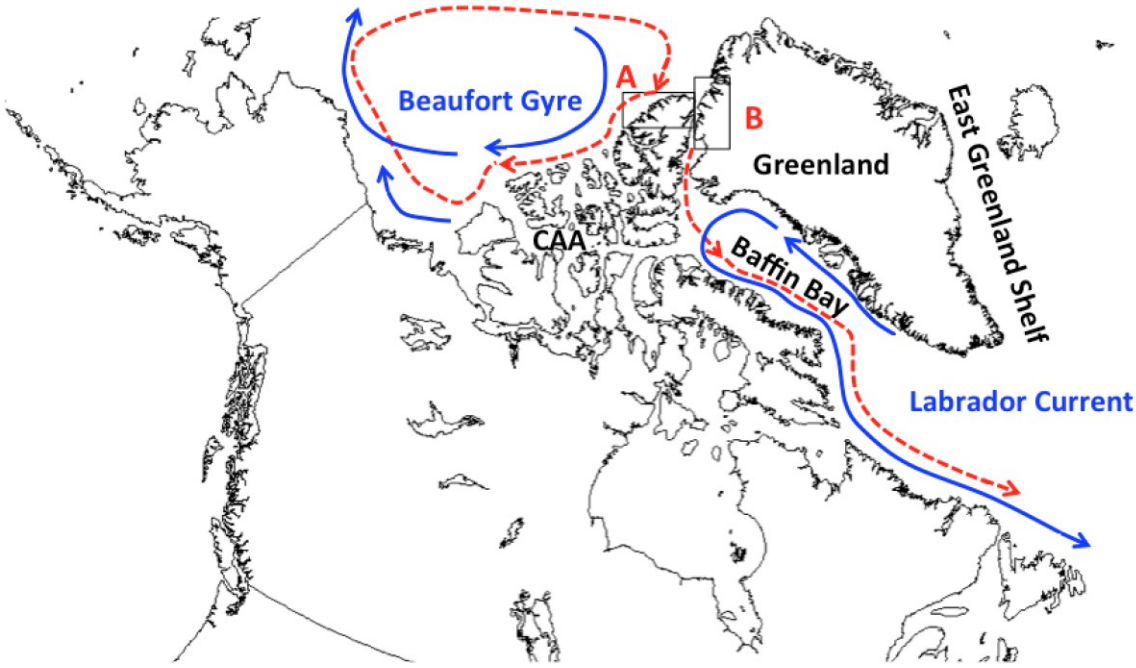


**Figure 2.1 Common drift patterns of ice islands, shown in red (dashed lines), originating from Northern Ellesmere Island ice shelves in the Canadian Arctic Archipelago (CAA) (A), as well as northwest Greenland floating glacier tongues (B). The water current direction of the Baufort Gyre and Laborador Current are shown in blue (solid lines) (adapted from Crawford, 2013).**

Ice shelf growth occurs by annual snow accumulation, basal freezing, and by the seaward extension of land glaciers (Jeffries 1992). Calving of an ice shelf or floating glacier tongue is thought to occur due to persistent winds, tidal action and/or pressure from the surrounding ice pack (Koenig et al. 1952). Currently, Arctic warming is increasing the frequency of ice shelf and floating glacier tongue calving events (AMAP 2011; Copland et al. 2007). Sea ice acts as a barrier to wind and wave action, therefore, the recent reductions in sea ice extent permit calving events, such as the 2005 calving of Ayles Ice Shelf, Ellesmere Island (Copland et al. 2007). Additionally, it has been suggested that positive Arctic surface air temperature anomalies since 2000, relative to both the 1971-2000 and 1981-2010 baseline periods (Overland et al. 2012), are associated

with ice shelf and floating glacier tongue calving events (Copland et al. 2007; Peterson 2005).

Deterioration processes, including the fracturing of an ice island into two or more pieces, can produce fragments that are similar to icebergs. The deterioration of icebergs is caused by surface melting and evaporation, wave induced erosion, calving from the sides, and fracturing into two or more pieces (Kristensen 1983). Wave-induced erosion is observed at the waterline and results in the calving of overhanging ice cliffs (Kristensen 1983). This deterioration process typically accounts for the greatest proportion of iceberg deterioration (Savage 2001). Another reason for iceberg calving is from buoyant convection, where the low-density iceberg meltwater rises along the side of the iceberg, displacing the colder denser ocean water (Donaldson 1978; Huppert and Turner 1980; Savage 2001). This allows for the convection of heat from the water to the surface of the iceberg and promotes melting along the submerged sidewall.

### 2.2.1 Interactions between icebergs and the surrounding marine environment

The presence of an iceberg can interfere with ocean density and cause anomalies in three possible ways (Stephenson et al. 2011) (Figure 2.2). A narrow region of iceberg meltwater can rise along the iceberg keel, forming a buoyant convection cell (Horne 1985; Stephenson et al. 2011). This results in mixing between the meltwater and the surrounding seawater, thereby causing the marine deep water to rise (Donaldson 1978; Huppert and Turner 1980; Helly et al. 2011). Adjacent to the inner boundary layer of rising meltwater there exists an outer boundary layer of downwelling due to cabbelling (Garrett and Horne 1978). Cabbelling results when two water bodies of different densities combine to form a new water body with a higher density. Rising and descending waters

will remain at a depth of equal density to that of the far-field water (Stephenson et al. 2011). As a result, water commences to move away from the iceberg forming a series of nearly horizontally-oriented layers adjacent to the iceberg, where each layer is separated by a relatively thin interface. In water where this interleaving structure is present and vertical mixing is negligible, double-diffusive convection can occur. Double-diffusion can be identified in the hydrographic profiles by thermohaline staircases (Stephenson et al. 2011).

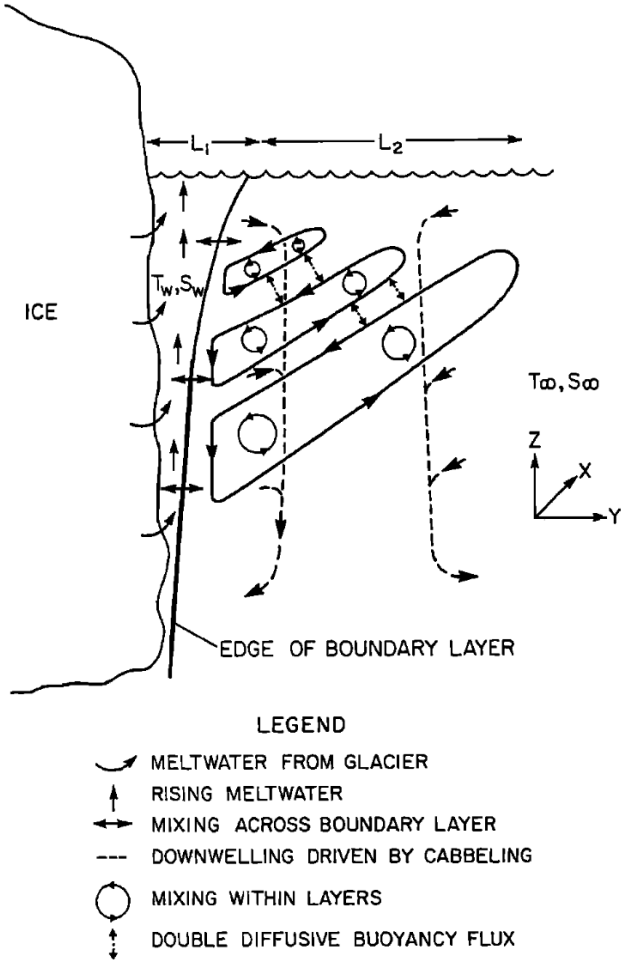


**Figure 2.2 Sketch of the density anomalies that occur in the water column adjacent to an iceberg. The inner boundary layer ($L_1$) consists of rising melt water and upwelling due to the formation of a buoyant convection cell. Once the rising meltwater reaches a level of neutral density it commences to move horizontally and is entrained into the outer boundary layer ($L_2$). Downwelling due to cabbelling and double-diffusive convection occur in $L_2$ (Horne 1985).**

Stern et al. (2015) suggested that ocean density anomalies adjacent to an iceberg might not only be the result of melting but could also be influenced by the prevailing wind direction. The net movement of water currents is the balance between Coriolis and turbulent drag forces from wind action (Price et al. 1987). Due to Ekman transport, the direction of the water currents is 90° to the right of the surface wind direction in the Northern Hemisphere and 90° to the left in the Southern Hemisphere. Therefore, a grounded iceberg could experience upwelling to the right of the wind direction (in the Northern Hemisphere) due to the movement of the surface waters away from the iceberg. This upwelling is distinct from the upwelling driven by a buoyant meltwater plume (Neshyba 1977; Helly et al. 2011; Stephenson et al. 2011). On the upstream side (left of the wind vector in the Northern Hemisphere), surface waters pile up against the iceberg, causing a sharpening of the density gradient at the base of the thermocline (Stern et al. 2015).

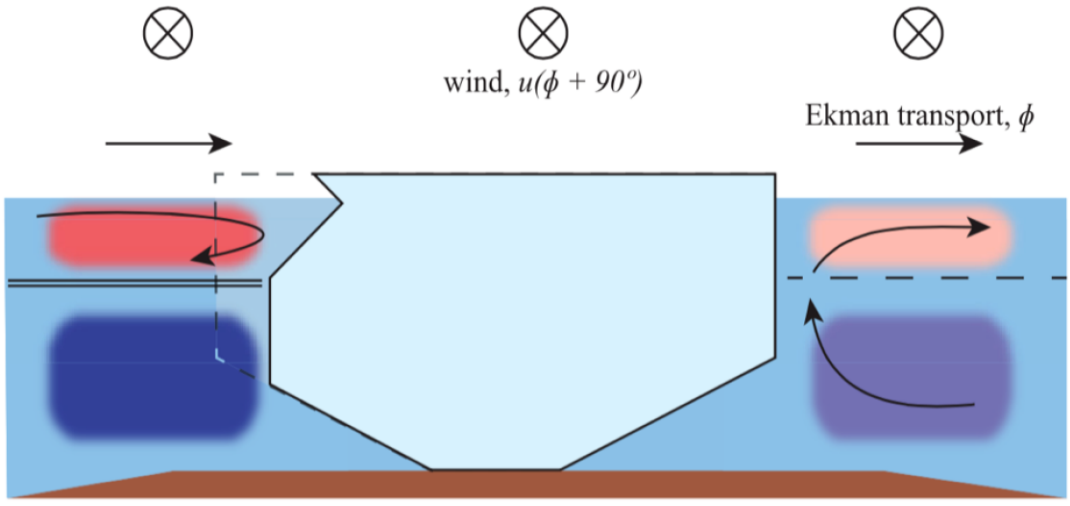


**Figure 2.3 Schematic of the wind-induced effects on hydrographic patterns adjacent to a grounded iceberg (in the Northern Hemisphere). The wind vector is into the page. To the right of the wind vector, upwelling and the transport of water away from the iceberg causes the mixed layer to become cooler and more saline. To the left of the wind vector, transport towards the iceberg causes warm fresh waters to pile up against the iceberg, resulting in a sharpening of the pycnocline (Stern et al. 2015).**

## 2.3 Primary production processes

Arctic continental shelves are important areas for primary production and account for most of the marine primary productivity in the high Arctic (Sakshaug 2004, Arrigo and Van Dijken 2015). The CAA represents over 50% of the total Arctic continental shelf area (Jakobsson et al. 2004), making it an important location for Arctic Ocean primary production (Sakshaug 2004, Apollonio and Matrai 2011). Phytoplankton growth is primarily dependent on light, temperature, and the supply of nutrients, whereas loss is mainly due to grazing by pelagic herbivores and sedimentation (Reynolds 2006).

Major macro-nutrients supporting phytoplankton growth include: nitrogen, phosphorus, and silicon (Chester 2003). Although there are exceptions (Martiny et al. 2013; Sterner et al. 2008), the Redfield ratio (C:N:P of 106:16:1 mol:mol) provides general stoichiometric relationships for the elemental composition of suspended material when neither nitrogen or phosphorus is growth-limiting (Redfield et al. 1963). In the Arctic Ocean, nitrogen is often considered the limiting nutrient for primary production (Apollonio and Matrai 2011; Tremblay and Gagnon 2009) and the primary control of the net annual yield of primary producers (Tremblay et al. 2002, 2006; Walsh et al. 2004).

At high latitudes, the extreme seasonality in light availability is the dominant controlling factor that constrains Arctic photosynthetically-derived primary production (Leu et al. 2015). The presence of seasonal or permanent sea ice, and especially snow-covered ice, further limits the penetration of light into the ocean (Bergmann et al. 1991; Mei et al. 2002). During the winter months, no (or very limited) light is available for photosynthesis (Leu et al. 2015). A phytoplankton bloom can typically commence only after the sea ice has reached an advanced state of melt and disintegration (Arrigo et al.

2012; Fortier et al. 2002; Mundy et al. 2014). At 75°N, the latitude of Resolute, Nunavut and the region of focus in this study, the polar night extends from the second week of November to the first week of February. In Barrow Strait, the break up of the sea ice typically occurs during the month of July and high phytoplankton biomass occurs in July-early August (Michel et al. 2006, Apollonio and Matrai 2011).

As the result of sea ice meltwater, there is an increase in water column stratification which favours the maintenance of phytoplankton cells in the sunlit surface layer; however, the formation of a strong pycnocline produces a barrier that prevents the transportation of nutrients above the pycnocline (Carmack and Wassmann 2006; Carmack 2007). Throughout the progression of the bloom, the chl *a* maximum gradually deepens to the nutricline (Brown et al. 2015; Gradinger and Baumann 1991; Kattner and Becker 1991; Tremblay et al. 2008). The termination of a phytoplankton bloom is typically the result of nutrient depletion in the surface waters (e.g., Sakshaug 2004).

Vertical stratification can also influence phytoplankton community structure (e.g., diatom-based versus flagellate-based systems) (Ardyna et al. 2011; Carmack and Wassmann 2006; Li et al. 2009). Diatom-based systems, primarily composed of large phytoplankton cells are favoured in conditions of high nutrient concentrations and are typically supported by new nitrogenous nutrients in well-mixed waters (Tremblay et al., 2002; Ardyna et al., 2011). These systems are considered to be efficient in transferring energy to upper trophic levels and mass/carbon to deeper waters (Fenchel 1988; Cushing 1989). In the CAA, productive diatom-based systems have been described for different well-mixed eutrophic waters in Baffin Bay, Lancaster Sound and the Amundsen Gulf hotspot (Ardyna et al., 2011).

In contrast, flagellate-based systems are characterized by smaller cells such as picophytoplankton (< 2 μm), and autotrophic, heterotrophic or mixotrophic nanoflagellates (< 5 μm, Azam et al., 1983, Landry et al., 1997). Flagellate-based systems typically support longer food chains than diatom-based systems, and therefore provide less export to higher trophic levels (Fenchel 1988; Cushing 1989). The large surface-area-to volume ratio of small cells provides for effective acquisition of nutrients in environments with low nutrient supply (Li et al. 2009). Therefore, flagellate-based systems are competitive in stratified environments such as the Beaufort Sea and central region of the CAA, and can be supported by regenerated nutrients (Carmack et al. 2004; Simpson et al. 2008; Tremblay et al. 2009). In contrast, diatom based systems are mainly fuelled by new nitrogenous nutrients that are found in well-mixed waters (Ardyna et al. 2011; Garneau et al. 2007; Tremblay et al. 2002).

### 2.4 Biological processes associated with icebergs

In the Antarctic, icebergs in the open ocean have been associated with relatively high biological activity and have been described as 'hot spots' of chemical and biological enrichment (Smith et al. 2007). In the Antarctic, icebergs can lift nutrient limitation in the photic zone in two ways: by directly contributing nutrients through iceberg meltwater (Smith et al. 2007), or by causing upwelling of nutrient-rich deep waters (Neshyba 1977; Horne 1985; Stephenson et al. 2011). The upwelling water adjacent to the iceberg will only rise until it reaches a level of neutral density, here it commences to move horizontally, forming a series of layers separated by a relatively thin layer of ambient seawater (Huppert and Turner 1980). This processes results in double-diffusion (convection along two gradients, one of salinity and the other of temperature), which has

been suggested by Stephenson et al. (2011) to provide a means for upwelling of nutrients over a much larger area than from turbulent upwelling.

A few Antarctic studies have observed the occurrence of these iceberg associated 'hot spots' (e.g., Schwarz and Schodlok 2009; Smith et al. 2007; Vernet et al. 2011; Duprat et al. 2016) and, to date, there have been no similar studies in the Arctic. An extensive study of the bio-chemical conditions near an iceberg in the Antarctic determined that phytoplankton biomass was lower in the immediate vicinity of the iceberg (<0.2 km) compared to further away (Smith et al. 2007). This was attributed to upwelling adjacent to the iceberg, resulting in phytoplankton displacement and a lagged increase in productivity in the iceberg's wake (Helly et al. 2011; Schwarz and Schodlok 2009). Moderate phytoplankton biomass was observed <0.25 km from the iceberg and the highest biomass were observed around 0.5 km away (Smith et al. 2007). At distances >1.0 km from the iceberg, phytoplankton biomass declined to background values due to the dispersion or uptake of the nutrients.

In the Antarctic, icebergs contain biologically important micronutrients such as iron (Lin et al. 2011; Smith et al. 2007). While iron is a limiting nutrient in the Antarctic, it is not considered limiting in the Arctic, where nitrogenenous nutrients, in particular nitrate, are typically the limiting on continental shelves (Apollonio and Matrai 2011; Tremblay and Gagnon 2009). While the surface waters in the CAA are typically very low or depleted in $NO_3^-$ (<1.5 μmol $L^{-1}$) by mid-August (Apollonio and Matrai 2011), Arctic icebergs are not expected to be a significant source of nitrate. For example, average nitrate concentrations in a Greenland glacier (Tung et al. 2006) and in an iceberg in the NW Weddell Sea (Vernet et al. 2011) were 0.62 μmol $L^{-1}$ and 0.32 μmol $L^{-1}$,

respectively. Higher nitrate concentrations were observed in the melt ponds on the surface of the Serson (1.0 μmol $L^{-1}$) and Markham ice shelves (1.9 μmol $L^{-1}$), at the northern coast of Ellesmere Island, Nunavut (Mueller et al. 2006). Since this is a benthic environment with enhanced microbial activity, these concentrations may be considered as upper bounds.

# 3 Chapter: Methods

## 3.1 Study site

In August 2014, water column sampling was carried out in the vicinity of a grounded iceberg fragment near Resolute, Nunavut. The iceberg was located at 74.614°N, 94.729°W on August 11$^{th}$ and moved approximately 200 m in a southeast direction between August 12$^{th}$ and 15$^{th}$ (74.619°N, 94.707°W; Figure 3.1). The iceberg was approximately 230 m long by 160 m wide with a draft of 70 m and a maximum freeboard of 20-25 m.

The break up of sea ice in Resolute Passage typically occurs in July, while freeze-up begins in Resolute Bay in September and extends offshore by late October (http://iceweb1.cis.ec.gc.ca/30Atlas/page1.xhtml?region=AR&lang=en). Barrow Strait is a high-energy area, with diurnal tides up to 2 m and current velocities up to 60 cm $s^{-1}$ near Resolute (Cota et al. 1987).

## 3.2 Sampling and data collection

Sampling stations were distributed along two perpendicular transects oriented east-west (E-W) and north-south (N-S), with stations being closer in proximity to each other near the iceberg (Figure 3.2). On each transect, stations were identified numerically in ascending order based on their distance from the iceberg. The 42 stations in the study were partitioned into three different types: 13 CTD (Conductivity Temperature Depth) stations, 22 spatial survey stations, and seven full stations. A summary of CTD profiling and water column sampling on each sampling day can be found in Appendix A. CTD profiles were obtained at all stations using an Idronaut CTD, model 304. At the spatial survey stations surface water was sampled using 2 L Niskin bottles immediately after

CTD profiling. At each station, sub-samples were collected on site for salinity, $\delta^{18}O$ and nutrient analyses. In addition, for a subset of seven spatial survey stations, surface water samples were kept in clean Nalgene bottles and brought back to the shore laboratory for dissolved organic carbon (DOC), protist abundance as well as chlorophyll *a* (chl *a*) analyses (see Fig. 3.2 for station locations). The full stations included *in-situ* fluorescence profiling using a Turner C3 submersible fluorometer and water sampling (2 L Niskin bottles) at the surface, 5, 10, 25, and 50 m depths. Sub-samples were collected on site for salinity, nutrients (nitrate + nitrite ($NO_3^-$ + $NO_2^-$), phosphate ($PO_4^{3-}$) and silicic acid ($Si(OH)_4$), DOC, as well as protist abundance. The remainder of the samples were transferred to clean Nalgene bottles, kept cold and dark, and were brought back to a shore laboratory for further processing and analysis of chl *a*. Due to the low concentration of $NO_2^-$ in the water samples, from here on, $NO_3^-$ + $NO_2^-$ will be referred to as $NO_3^-$.

In addition to these three stations types, end member properties were measured at a coastal marine station as well as for six ice samples from the iceberg (Figure 3.1). The end member properties of the collected samples included: salinity, $\delta^{18}O$, nutrients, DOC and protist abundance. The coastal marine end member sample was collected at 110 m depth at a station located 8 km south (offshore) of the iceberg. The iceberg was sampled at two different locations as high as possible (~1.5 m) above the waterline to ensure the least amount of seawater contamination. The sampling equipment was cleaned with 90% ethanol and ~ 1 L per sample of ice was chipped into sterile bags (Whirl-Pack, NASCO) which were kept cold and dark until further processing and analysis in the laboratory.

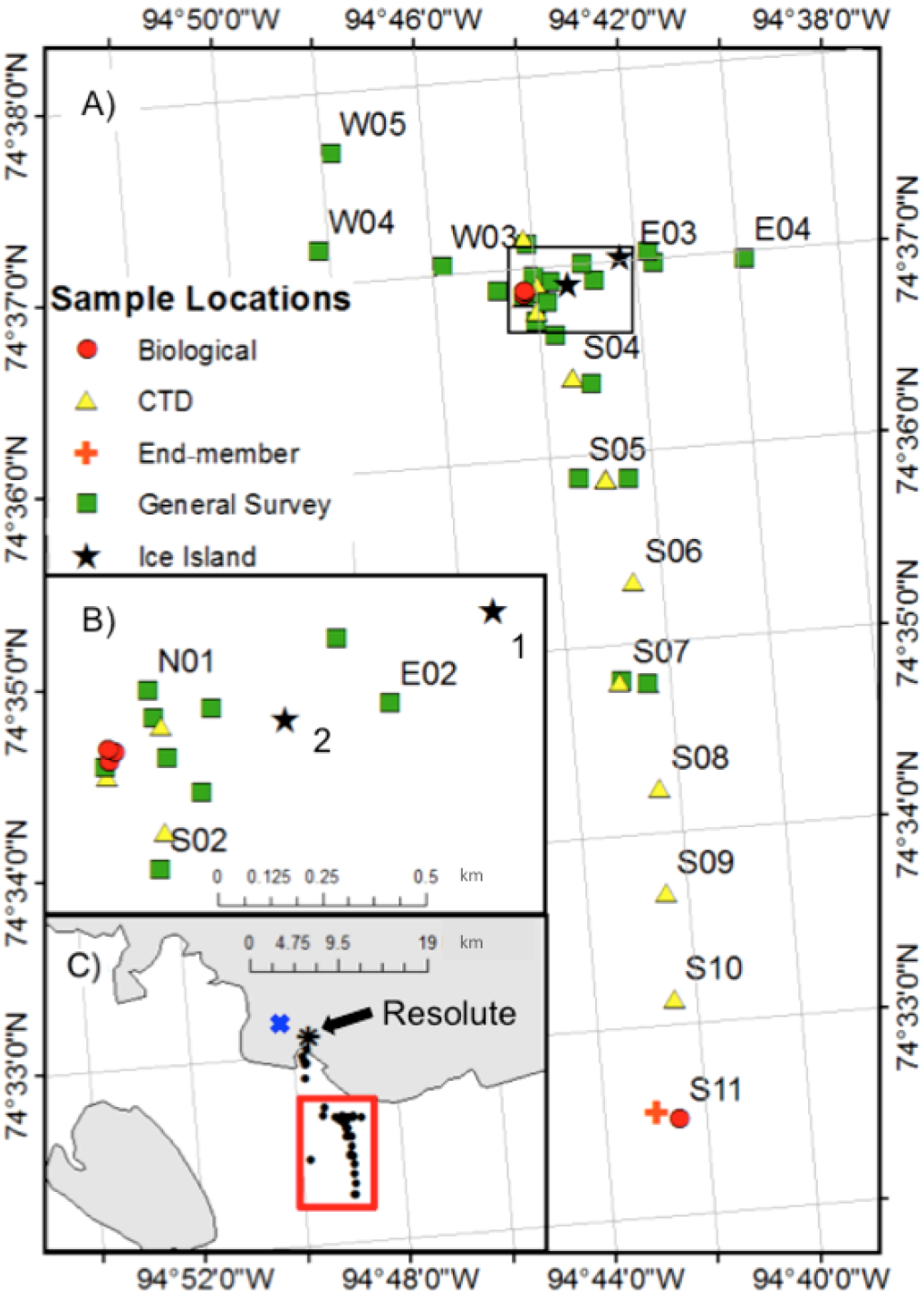


**Figure 3.1 All stations visited from August 11th to 29th, 2014 with sampling transects named in terms of nominal direction: east to west (E-W) and north to south (N-S) (A) as well as a close up of the stations next to the iceberg (B) and the general Resolute Passage area (C). Sampling stations were partitioned into three types: conductivity temperature depth (CTD) (yellow triangle), spatial survey (green square), full stations (red circle) and end-members (orange cross). End-member samples were also gathered from the iceberg. The iceberg location, before (1) and after (2) drifting is indicated by the stars. A black asterisk and blue 'X' indicate the location of the Hamlet of Resolute and the weather station, respectively.**

## 3.3 Profiling, subsampling and laboratory methods

### 3.3.1 Profiling

The CTD downcast profiles were used for analysis, with depth measured in meters, converted from pressure. Conductivity measurements were converted into salinity using the UNESCO equation (Fofonoff and Millard 1991).

### 3.3.2 Nutrients

Samples for nutrient determination were collected into acid-cleaned cryovials directly from the Niskin bottle after rinsing three times. Samples were kept in a cooler on ice during transportation to the laboratory, where they were frozen at -80°C. Samples were analyzed on a Bran+Luebbe AutoAnalyzer 3 for $NO_3^-$, $PO_4^{3-}$ and $Si(OH)_4$ using standard colorimetric methods (Grasshoff et al. 1999). The $NO_3^-$, $PO_4^{3-}$ and $Si(OH)_4$ detection limits are 0.051, 0.003 and 0.064 μmol $L^{-1}$, respectively.

### 3.3.3 $\delta^{18}O$

Duplicate $\delta^{18}O$ samples were collected in borosilicate acid glass scintillation vials in the shore laboratory by subsampling water collected in the field. During transportation to the shore laboratory the Nalgene bottles were kept dark and cold in a cooler. In the laboratory, the samples were kept at 4°C until analysis. $\delta^{18}O$ measurements were obtained by cavity ring-down laser-based spectroscopy (CRDS) using a Los Gatos Research Inc. Laser Water Isotope Analyzer (LWIA). Samples were inserted into the instrument using an autoinjector and evaporated for isotopic analysis. The equation for calculating $\delta^{18}O$ (‰) is as follows:

$$\delta^{18}O = \frac{\left(\left(^{18}O/^{16}O\right)_{Sample} - \left(^{18}O/^{16}O\right)_{Standard} - 1\right) \times 1000}{\left(^{18}O/^{16}O16\right)_{Standard}}, \qquad \text{Eq 3.1}$$

where the $(^{18}O/^{16}O)_{Standard}$ was obtained from Vienna Standard Mean Ocean Water (VSMOW2). Each sample and working standard was injected 12 times; the first nine injects were discarded due to memory effects while the last four injections were averaged. The mean of the standard deviations for the replicate measurements was 0.16‰. Between batches of 30 samples, the injector block, transfer tube, and septum support were cleaned thoroughly by ultrasonication to reduce salt contamination and minimize the memory effect between samples (Berman et al. 2013).

### 3.3.4 Dissolved organic carbon

Duplicate samples for DOC determination were filtered through pre-combusted (450°C for 5 h) Whatman GF/F 25 mm filters. The filtrate was stored in acid-washed pre-combusted amber sample vials with Teflon caps. Samples, acidified with 50% (v:v) phosphoric acid, were kept in the dark at 4°C until analysis. DOC was determined using high-temperature catalytic combustion on a Shimadzu TOC-VCPH analyzer with an ASI-V auto sampler (Knap et al. 1996). Standards prepared with potassium hydrogen phthalate acid (KHP) were used for calibration of DOC measurements (Knap et al. 1996). Results were systematically checked against low-carbon water (2 μM) and deep Sargasso Sea reference water (44–47 μmol $L^{-1}$), produced by the Hansell's certified reference materials program (http://www.rsmas.miami.edu/ groups/biogeochem/CRM.html).

Flow cytometry was used to determine protist (i.e., pico- and nanoeukaryote) abundance according to Belzile et al. (2008). Duplicate sub-samples were preserved with glutaraldehyde (0.1% v:v final concentration) and stored at −80°C until analysis. For the analysis, subsamples were stained with SYBR Green I (0.1% v:v final concentration; Molecular Probes) and counted with an Epics Altra flow cytometer (Beckman Coulter)

equipped with a 488 nm laser (15 mW output). Microspheres (1 μm, Fluoresbrite plain YG, Polysciences) were added to each sample as an internal standard.

### 3.3.5 Salinity

Salinity samples were kept in clean polycarbonate bottles and kept at 4ºC until analysis on a Portasal 8410A (Guildine Instruments) salinometer. Salinity measurements were systematically checked against International Association for the Physical Science of the Oceans seawater standards.

### 3.3.6 Chlorophyll *a*

Chl *a* concentrations were determined using fluorometric methods described by Parsons et al. (1984). Duplicate sub-samples were filtered onto Whatman GF/F or 5 μm Nuclepore polycarbonate membrane filters to determine chlorophyll *a* total ($Chl_{TOT}$) and chlorophyll *a* from cells >5 μm ($Chl_{5\ \mu m}$) respectively and extracted in 90% acetone for 24 h at 4°C in the dark. Fluorescence was measured before and after acidification with 5% hydrochloric acid (HCl) on a Turner Designs model 10-AU fluorometer calibrated using pure chl *a* extract (Sigma-Aldrich). Duplicate $Chl_{TOT}$ and $Chl_{5\ \mu m}$ samples were averaged. Total water column chl *a* measurements (mg chl *a* $m^{-2}$) were computed from sample concentrations at discrete depths using trapezoidal integration.

## 3.4 Environmental conditions

Climate data, tide tables, and sea ice charts were obtained for the month of August 2014 for Resolute, Nunavut. Hourly climate data for Resolute (including air temperature and pressure, sky conditions, wind speed and direction) were obtained from an Environment Canada weather station located at 74.72°N, 94.97°W, ~14 km to the northwest of the iceberg (http://weather.gc.ca/). Sky conditions were given as either clear

(0 tenths), mainly clear (1 to 4 tenths), mostly cloudy (5 to 9 tenths) or cloudy (10 tenths). Hourly wind speed and direction were averaged into daily measurements. Hourly tide tables were obtained from Environment Canada (http://www.waterlevels.gc.ca/) and the change in tidal height over each sampling period was determined. Daily sea ice charts for Resolute Passage were obtained from the Canadian Ice Service (CIS) in digital format (http://iceweb1.cis.ec.gc.ca/). The sea ice charts represent an estimate of the ice conditions and are charted using the World Meteorological Organization (WMO) egg code, which provides information on sea ice concentration measured in tenths, stage of development or ice type, and floe size or form of development (MANICE 2005). Using the egg code, the sea ice concentration at the location of the iceberg was determined in percent. For the purpose of this study, an egg code sea ice coverage of 9+ was assigned a coverage of 95%.

### 3.5 Physical oceanographic calculations and statistical analysis

Data were analyzed using R Project for Statistical Computing software and Ocean Data View software. Ocean Data View was also used to generate gridded temperature and salinity plots (Schlitzer 2015). Depending on the normality of the data, either a Wilcoxon rank sum test or a t-test was used to infer if groups of samples were significantly different, such as the comparison between the upper and lower water column or adjacent to (30 m) and far from (>30 m) the iceberg.

Multiple minor pycnoclines were detected in all of the profiles in the study area. Each profile was inspected visually to examine the various pycnoclines; the main pycnocline was defined as the first occurrence below 5 m depth where the gradient in density was greater than >0.02 (kg $m^{-3}$) $m^{-1}$, following Ardyna et al. (2011). The lower

water column was defined as below this main pycnocline and the upper water column was above. This method produced pycnocline depths ranging from 7 to 30 m. The surface layer of the water column was defined as the upper 1-4 m of the water column.

Freshwater from a melting iceberg rises to a point of neutral density in the water column and this creates a stepped profile where isopycnal layers are interspersed within the original density profile (Stephenson et al. 2011; Jacobs et al. 1981; Huppert and Turner 1980). An estimate of the theoretical thickness of layers of uniform density, $h$ (m), can be derived with a semi-empirical equation that is valid for a wide range of temperature and salinity values in the ocean:

$$h = \frac{0.65\left[\rho\left(T_{fp}, S\right) - \rho\left(T\ , S\right)\right]}{d\rho/dz}\ , \qquad \text{Eq. 3.2}$$

where the numerator represents the difference in density of water $\rho$ (kg m$^{-3}$) at far-field salinity, $S$, at the depressed freezing point near the iceberg, $T_{fp}$ (°C), and the density of water at both far-field salinity, and temperature, $T$ (°C). The denominator is the far-field vertical gradient in density due to changes in salinity alone, $d\rho/dz$ (Huppert and Turner 1980). $d\rho/dz$ was computed using densities calculated from the salinity at 5 and 50 m depth along with the mean temperature at these two depths. $T_{fp}$ was calculated using the freezing point depression due to ambient salinity with the TEOS-10 library (IOC/SCOR/IAPSO, 2010). $T_{fp}$ was also used to calculate the driving temperature, or the difference between ambient and freezing water temperatures, as this provides a measure for the rate of ice melt (Jacobs et al. 1981).

Salinity and $\delta^{18}O$ served as end-member values in the three-component mixing model of coastal marine water (CMW), iceberg meltwater (IM) and sea-ice meltwater (SIM). The fractions (f) were calculated using the following mass balance equations,

$$f_{CMW} + f_{IM} + f_{SIM} = 1, \quad \text{Eq 3.3}$$

$$f_{CMW}\delta_{CMW} + f_{IM}\delta_{IIM} + f_{SIM}\delta_{SIM} = \delta, \quad \text{Eq 3.4}$$

$$f_{CMW}S_{CMW} + f_{IM}S_{IIM} + f_{SIM}S_{SIM} = S, \quad \text{Eq 3.5}$$

where $\delta$ and S refer to the measured values of $\delta^{18}O$ and salinity, respectively (Yamamoto-Kawai et al. 2010). The corresponding values for the mixing end members can be seen in Table 4.2.

# 4 Chapter: Results

## 4.1 Environmental conditions

From August 1st to 31st, the mean wind speed, surface air temperature and atmospheric pressure were 5.4 m $s^{-1}$ (0 to 18 m $s^{-1}$), 2.1°C (-1.8 to 9.6°C) and 101. 20 kPa (99.19 to 101.56 kPa), respectively (Figure 4.1). From August 2nd to 5th, the winds were southeasterly and averaged 5.2 m $s^{-1}$ (1.1 to 8.9 m $s^{-1}$). There was a sudden shift in wind direction and speed on August 6th, which coincided with an increase in air temperature. The winds were generally offshore (northerly) and wind speeds were elevated until August 18th, with an average speed of 6.2 m $s^{-1}$ (0 to 18 m $s^{-1}$). On August 20th the wind direction shifted to westerly and there was a decrease in air temperature and atmospheric pressure. This was followed by a sharp increase in atmospheric pressure on August 22nd, for several days, while the air temperature rose steadily to 5°C over the following week.

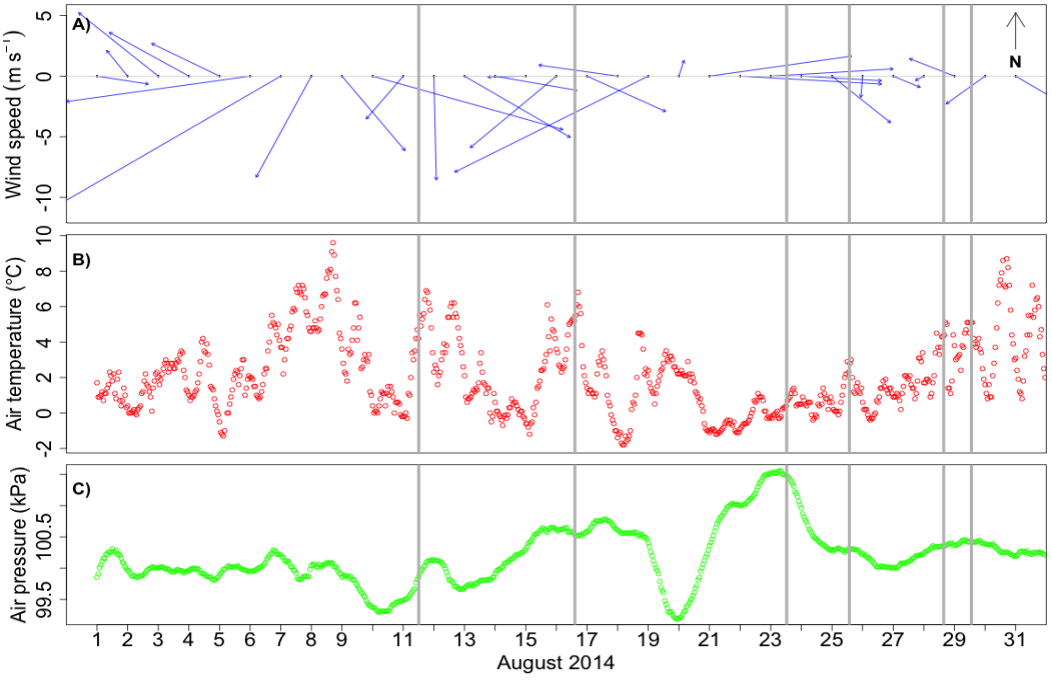


**Figure 4.1 Meteorological conditions near the study site. Wind speed (m $s^{-1}$) and direction (A), surface air temperature (°C) (B), and atmospheric pressure (kPa) (C), from August 1st to 31st, 2014. The coastline is oriented in the east to west direction. Vertical grey lines indicate sampling times.**

Tides near Resolute are mixed semidiurnal, having two high and low tides of different height in every lunar day. During August 2014, the highest tide occurred in the night, a low tide followed in the early morning, a smaller high tide occurred at mid-day and the lowest tide was in the evening (tidal range: 0.1 to 2 m). Table 4.1 provides the tidal height and cloud conditions during each sampling interval.

**Table 4.1 Sampling dates (dd/mm/yyyy) and start and stop times (hh:mm local time), cloud conditions and change in tide height (m) during the sampling periods. Rate of change in tide height was typically 0.17 m $h^{-1}$.**

| Date | Start time | Stop time | Cloud condition | Change in tide height (m) |
|---|---|---|---|---|
| 11/08/2014 | 12:07 | 16:42 | Mainly Clear | -0.9 |
| 16/08/2014 | 14:30 | 17:21 | Cloudy | +0.3 |
| 23/08/2014 | 12:30 | 17:13 | Fog | -0.7 |
| 25/08/2014 | 13:40 | 20:03 | Cloudy | -0.9 |
| 28/08/2014 | 15:35 | 19:49 | Cloudy | -0.9 |
| 29/08/2014 | 13:18 | 17:40 | Clear | -0.6 |

Sea ice coverage at the location of the iceberg oscillated between 50% and 95% from August 1st to 8th (Figure 4.2). A shift in winds on August 8th (Fig. 4.1) moved the sea ice offshore (south), such that the vicinity of the iceberg was ice-free (0%) until August 15th. From August 16th to 24th the sea ice advected into the sampling area and the spatial coverage was between 20 and 70% before it returned to 0% coverage after August 25th.

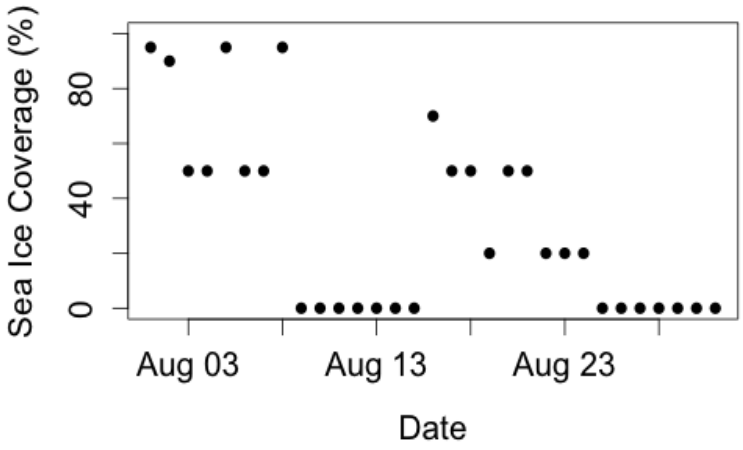


**Figure 4.2 Sea ice percent coverage at the iceberg location near Resolute from August 1st to 31st, 2014. Data were obtained from the Canadian Ice Service daily sea ice charts.**

## 4.2 Water characterization

### 4.2.1 Mixing model

The mixing model analysis indicates that all of the water samples were primarily composed of CMW (Figure 4.3). Waters between 50 and 80 m were the most similar to the CMW end-members, while surface waters were fresher and had more negative $\delta^{18}O$ values (Table 4.2). The $\delta^{18}O$ measurements in the upper and lower water column followed two distinct dilution lines; these lines had $R^2$ values of 0.64 and 0.85, respectively.

**Table 4.2 $\delta^{18}O$ and salinity end member properties for the coastal marine water (CMW), iceberg meltwater (IM) and sea-ice meltwater (SIM).**

| End-member | $\delta^{18}O$ (‰) | Salinity |
|---|---|---|
| CMW | -1.3 ± 0.7 | 32.9 ± 0 |
| IM | -31.4 ± 0.8 | 0 ± 0 |
| SIM | -0.38 ± -0.44* | 4 ± 1** |

*Values obtained from Christine Michel (pers. comm)
**Values obtained from Yamamoto-Kawai et al. (2010)

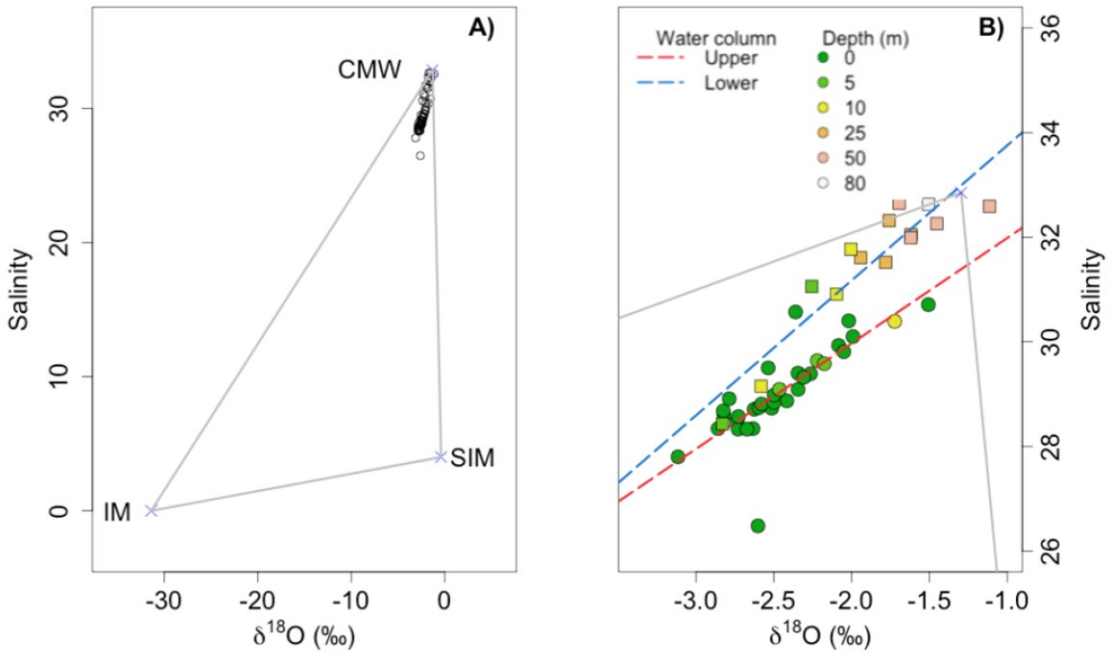


**Figure 4.3 Salinity versus $\delta^{18}O$ of coastal marine waters (CMW), iceberg meltwater (IM) and sea-ice melt (SIM) end-member values (A). Data points are coloured in terms of depth (0 to 80 m) and separated into the upper (circle) and lower (square) water column as detailed in the Methods in (B). Two dilution lines separate the upper (red) and lower (blue) water column. Note the low salinity outlier is likely representative of melting sea ice as it was sampled adjacent to a large floe.**

The mean $\delta^{18}O$ near (30 m) the iceberg was -2.09‰ (sd = 0.43) and the average $\delta^{18}O$ further (≥ 30 m) from the iceberg was -2.41‰ (sd = 0.43). There was no significant difference (W = 390, $p > 0.05$) between the $\delta^{18}O$ measurements near the iceberg (n = 20) compared to further away (n = 27). Additionally, the fraction of iceberg meltwater near the iceberg (mean = 2.3%, sd = 1.2%, n = 20) was not significantly different (W = 264, $p > 0.05$) compared to the meltwater fraction away from the iceberg (mean = 2.6%, sd = 1.6%, n = 27) (Figure 4.4).

$\delta^{18}O$ was more depleted in the upper water column (mean = -2.44‰, sd = 0.34, n = 34) compared to the lower water column (mean = -1.88‰, sd = 0.46, n = 13). A one-tailed t-test confirmed that the upper water column was significantly more depleted than the lower water column with respect to $\delta^{18}O$ ($t = 5.86$, $p < 0.001$). The three end-member

mixing model suggests a larger fraction of iceberg meltwater was found in the upper water column (mean = 3.2%, sd = 0.1, n= 34) compared to the lower water column (mean = 1.3%, sd = 1.4%, n = 13). Similarly, the fraction of SIM was higher in the upper water column (mean = 9.5%, sd = 2.3%, n = 34) compared to the lower water column (mean = 2.0%, sd = 2.9%, n = 13).

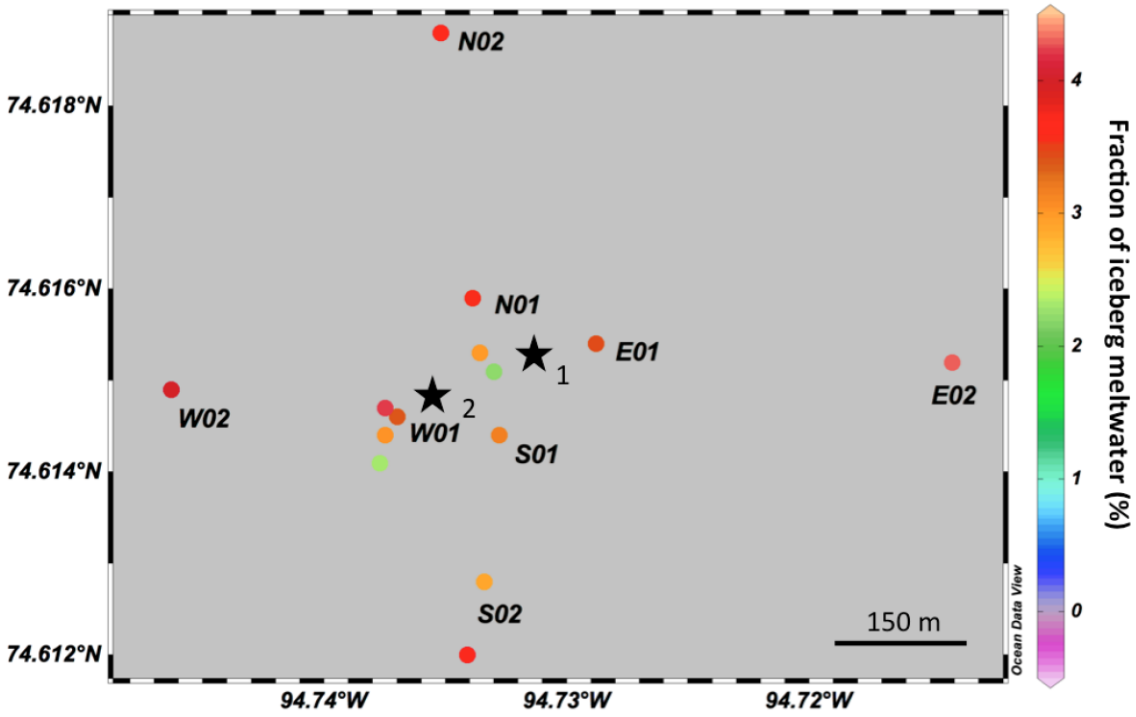


**Figure 4.4 Fraction of iceberg meltwater in surface waters of Resolute Passage, estimated using a three-component mixing model with $\delta^{18}O$ and salinity. The two positions of the iceberg are indicated by the stars.**

### 4.2.2 Typical oceanographic conditions

The temperature and salinity profiles in the study area typically showed a distinctive thermocline and halocline (pycnocline) separating the upper water column from the lower water column. The average depth of the pycnocline was 18.5 m (sd = 5.7, n = 42). Over the entire study area, excluding the water column adjacent (30 m) to the iceberg, the upper water column was significantly warmer (mean = -0.35ºC, sd = 0.29ºC)

than the lower water column (mean = -1.11ºC, sd = 0.24ºC) (W = 1720, p < 0.001). The upper water column was also significantly fresher (mean = 29.9, sd = 0.7) than the lower water column (mean = 32.2, sd = 0.2) (t = 19.545, p < 0.001).

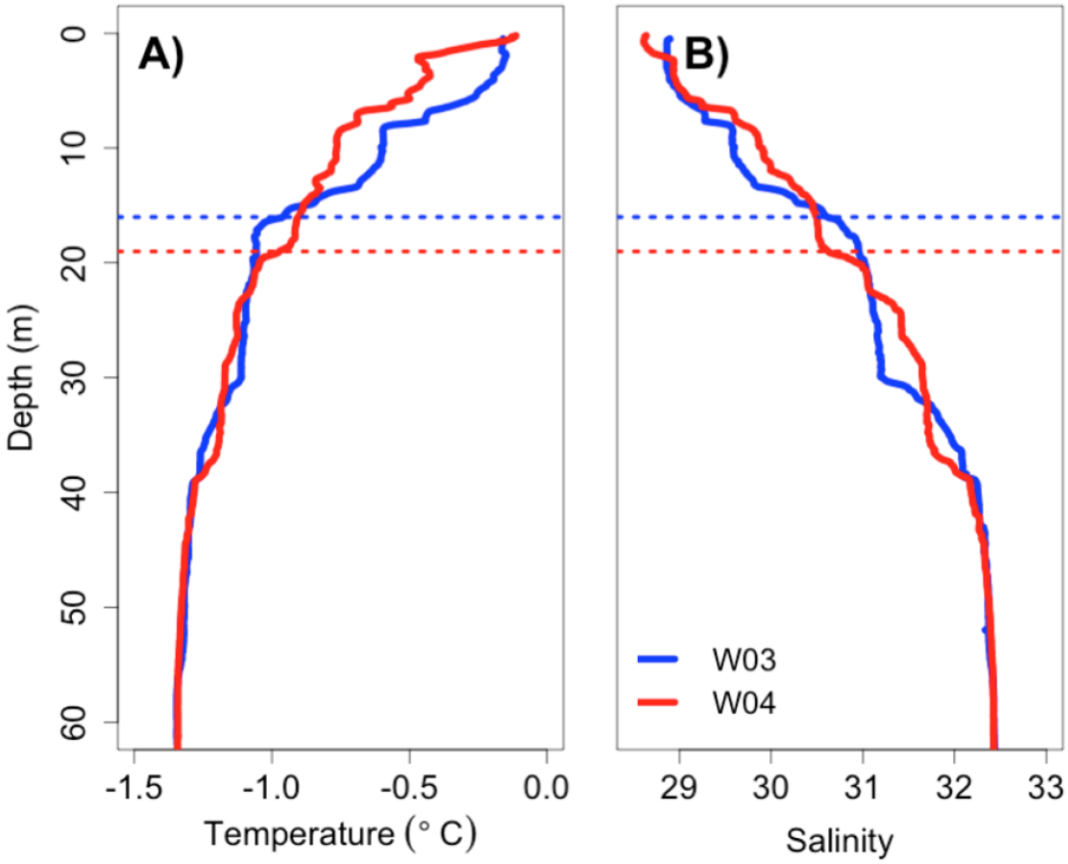


**Figure 4.5 Typical temperature (A) and salinity (B) profiles in the study area with the depths of the main pycnoclines (dashed lines). Profiles are from stations W03 and W04 on August 29th, 2014.**

### 4.2.3 N-S and E-W transects

Figures 4.6 to 4.9 are gridded plots of temperature and salinity along the N-S and E-W transects on August 11th, 2014. A distinctive warmer (-0.16ºC) and fresher (28.6) surface layer was observed at nearly all the stations (S01, S02, S03 and N02) along the N-S transect (Figures 4.6 and 4.7). The surface waters directly north of the iceberg (station N01) were colder (-0.36ºC) and more saline (29.1) than at all other stations. The

main pycnocline was at ca. 25 m depth at the northern stations (N01 and N02) and at ca. 10 m depth at the southern stations (S01, S02, and S03).

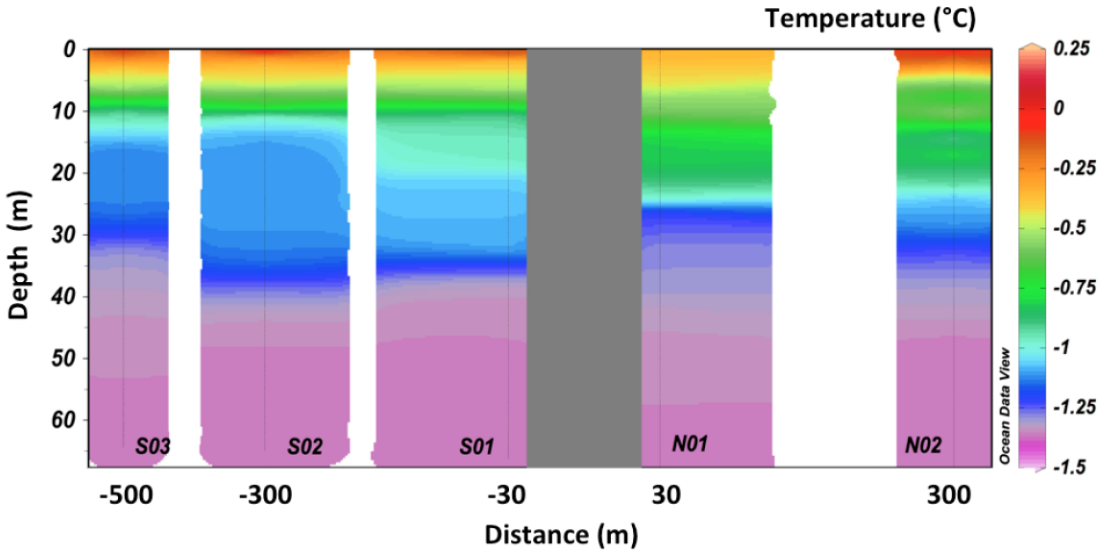


**Figure 4.6 Gridded temperature plot along the N-S transect, including stations S03, S02, S01, N01 and N02. The x-axis (log scale) shows distances from the iceberg. The grey area represents the approximate location of the iceberg.**

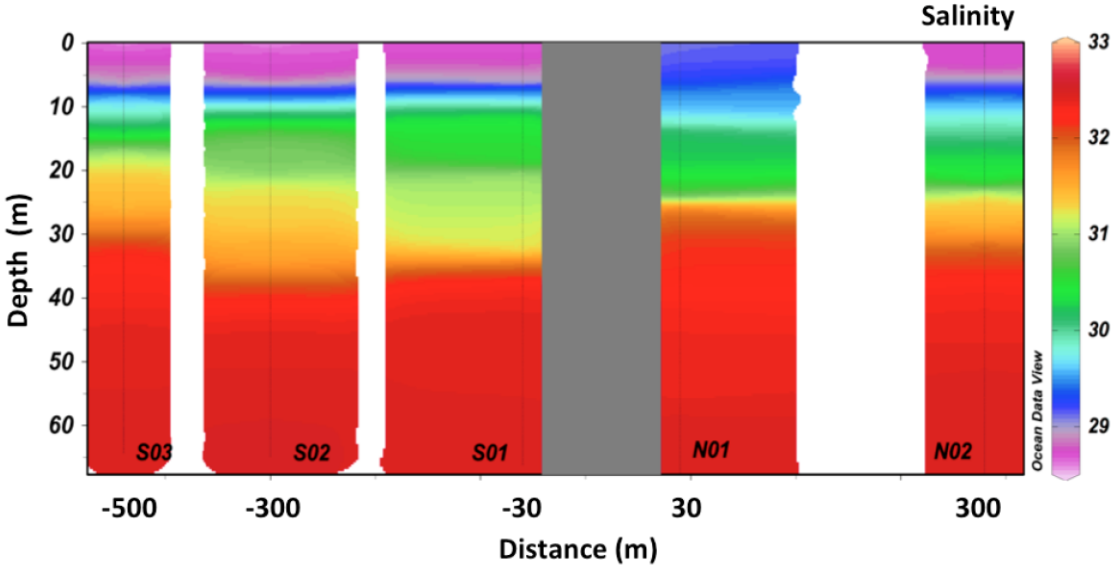


**Figure 4.7 Gridded salinity plot along the N-S transect, including stations S03, S02, S01, N01 and N02. The x-axis (log scale) shows distances from the iceberg. The grey area represents the approximate location of the iceberg.**

The E-W transect also showed variations in temperature and salinity with distance from the iceberg (Figures 4.8 and 4.9). The surface waters adjacent to the iceberg (stations E01 and W01) were colder (-0.44ºC) and more saline (28.8) compared to the stations further from the iceberg (W02, E02 and E03), which were warmer (0.60ºC) and fresher (28.4). The main pycnocline directly adjacent to the iceberg (stations E01 and W01) were deeper compared to those some distance away. Along the eastern and western transects the main pycnocline varied from ca. 20 to 23 m depth and ca. 12 to 25 m depth, respectively.

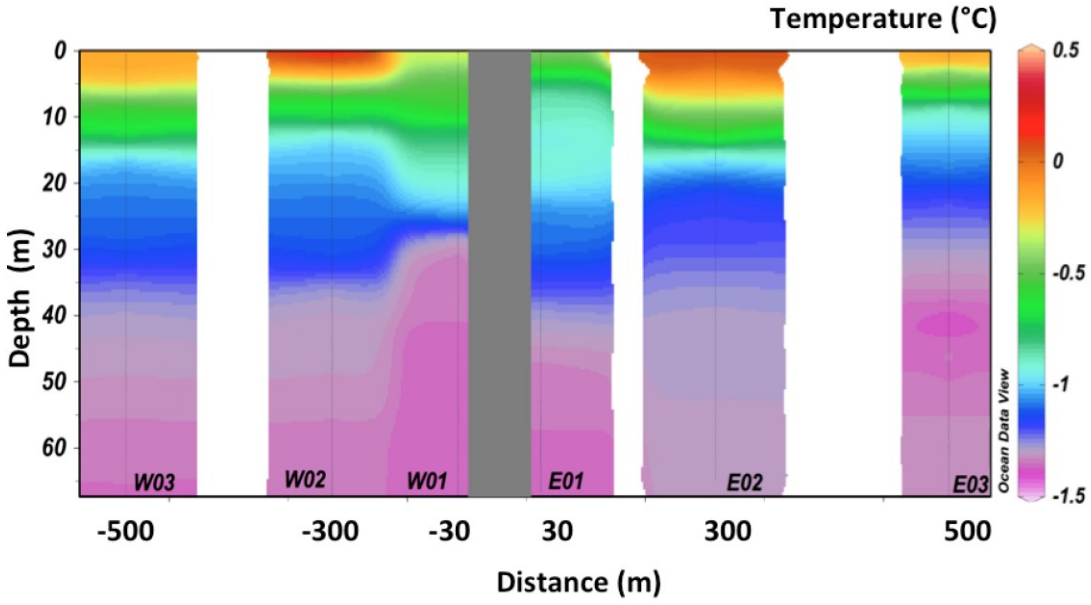


**Figure 4.8 Gridded temperature plot along the N-S transect, including stations W03, W02, W01, E01, E02 and E03. The x-axis (log scale) shows distances from the iceberg. The grey area represents the approximate location of the iceberg.**

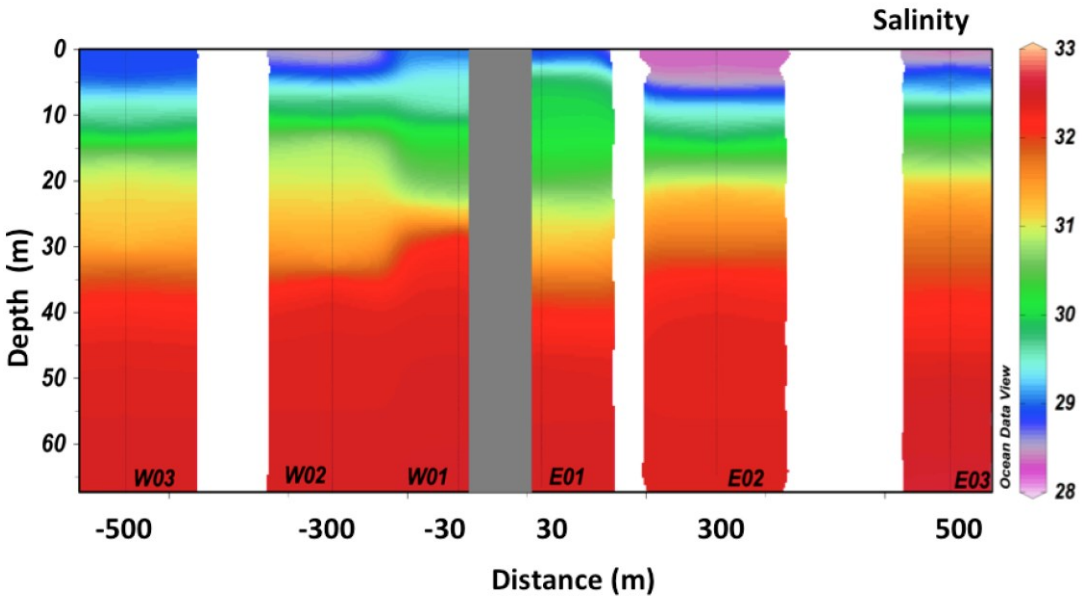


**Figure 4.9 Gridded salinity plot along the N-S transect, including stations W03, W02, W01, E01, E02 and E03. The x-axis (log scale) shows distances from the iceberg. The grey area represents the approximate location of the iceberg.**

### 4.2.4 Physical oceanographic conditions

The salinity and temperature profiles adjacent to the iceberg showed a series of themohaline density steps from the surface down to ca. 50 m depth (Figure 4.10). The main pycnocline at the stations directly adjacent to the iceberg were not significantly deeper compared to all other stations ($t = -1.973$, $p > 0.05$). Adjacent to the iceberg, the driving temperature in the upper water column (mean = 0.91ºC, sd = 0.08ºC) was significantly greater compared to the lower water column (mean = 0.48ºC, sd = 0.03ºC) ($t= 8.179$, $p < 0.01$). Station S08, located 5 km south the iceberg, had one shallow pycnocline at 7 m depth and very little evidence of thermohaline steps below this level (Figure 4.10). Station S08 represents the far-field or background water column conditions, which were used to predict the density steps that might result from iceberg melting (Huppert and Turner 1980). The predicted isopycnal layer thickness above the

main pycnocline at Station S08 was 0.5 m (Figure 4.10c). The thickness of the predicted isopycnal water layers decreased gradually from 7 to 50 m depth. However, adjacent to the iceberg, the observed isopycnal layer thicknesses at stations N01, E01, S01 and W01 ranged from 6.3 to 40 m, two orders of magnitude more than expected (Figure 4.10c).

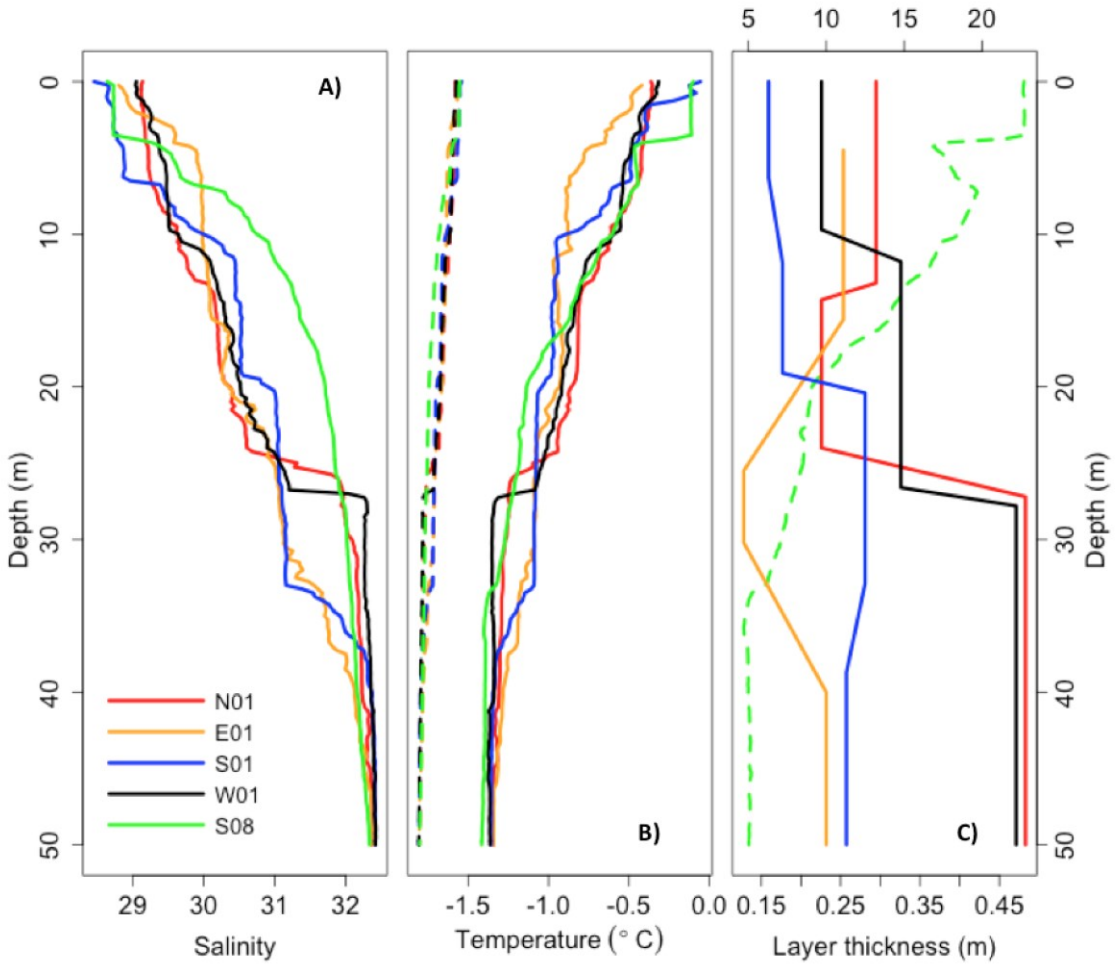


**Figure 4.10 Water column characteristics near the iceberg. Salinity (A), temperature (solid lines) and freezing point temperature (dashed lines) profiles (B). Data were taken at stations N01 (red), E01 (yellow), S01 (blue) and W01 (black) adjacent to the iceberg and station S08 (green) as representative of ambient conditions away from the iceberg on August 11th, 2014. Observed mixed layer thickness (solid vertical lines only, top axis) and predicted layer thickness from equation 3.2 using station S08 (dashed lines, bottom axis) (C).**

### 4.3 Chemical and biological variables

The concentrations of $NO_3^-$ ($t = 3.829$, $p < 0.001$), $Si(OH)_4$ ($W = 222$, $p < 0.001$) and $PO_4^{3-}$ ($t = 5.089$, $p < 0.001$) as well as the ratios of $NO_3^-$:$Si(OH)_4$ ($t = 4.525$, $p < 0.001$) and $NO_3^-$:$PO_4^{3-}$ ($t = 4.402$, $p < 0.001$) were significantly higher in the lower water column compared to the upper water column (Figure 4.11 and 4.12). The $NO_3^-$:$Si(OH)_4$ was consistently below the Redfield ratio while the opposite was observed with the $PO_4^{3-}$:$NO_3^-$ ratios.

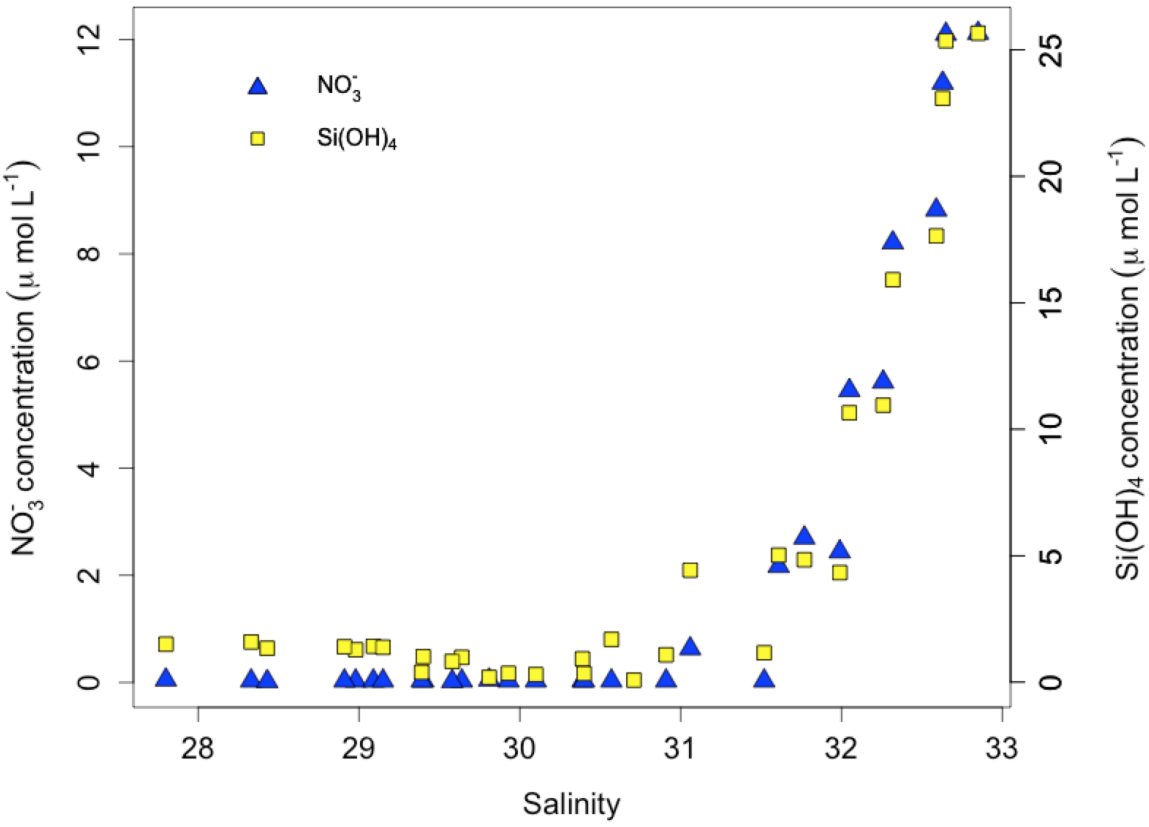


**Figure 4.11 Nitrate ($NO_3^-$) and silicic acid ($Si(OH)_4$) concentration versus water salinity in the study area.**

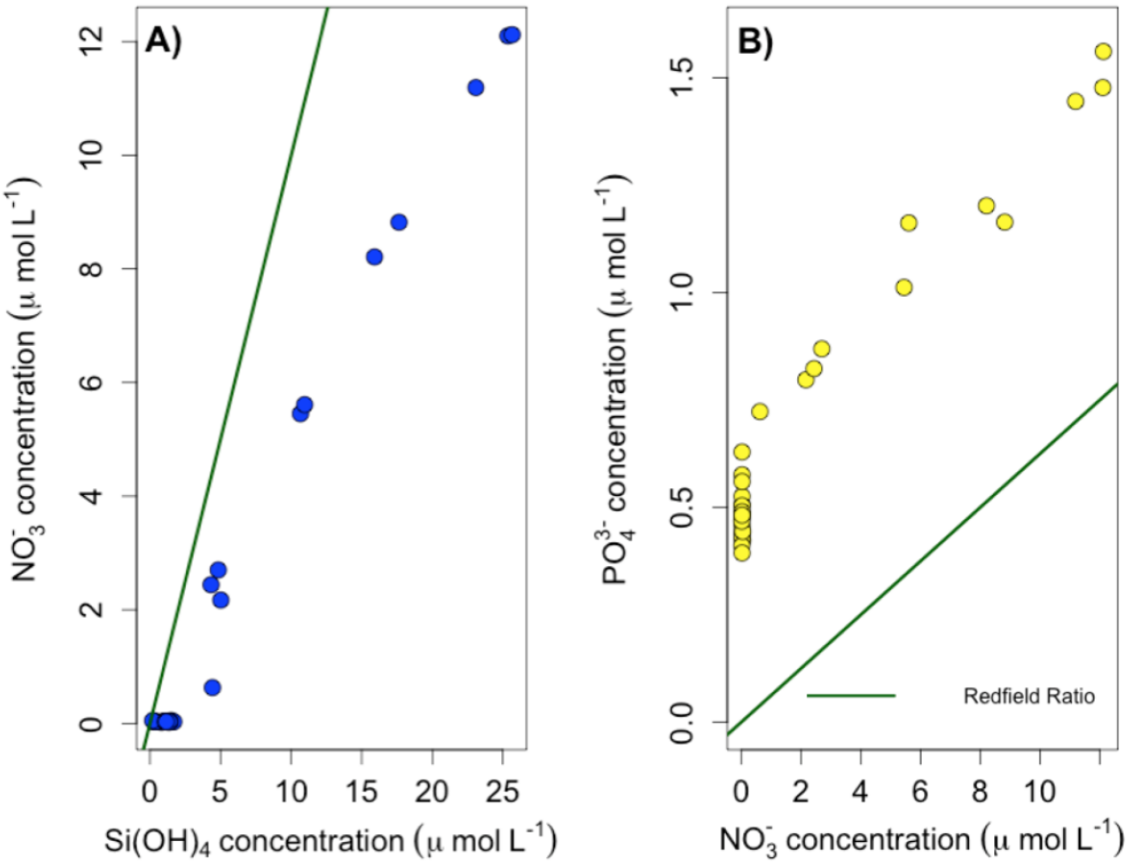


**Figure 4.12 Concentrations of nitrate ($NO_3^-$) versus silicic acid ($Si(OH)_4$) (A), as well as phosphate ($PO_4^{3-}$) versus nitrate ($NO_3^-$) (B) in the study area. The Redfield ratio is indicated by the green lines.**

A distinctive and extensive chl *a* subsurface maximum was observed at all stations in the study area and strengthened over the sampling period (Figure 4.13). The subsurface chlorophyll *a* maximum concentrations ranged from 13.7 to 21.0 mg $m^{-3}$. The average total water column chl *a* integrated over 50 m was 529 mg $m^{-2}$ (sd = 176, n = 4) for the sampling period. The *in situ* subsurface chl *a* maxima were also evident in the measured subsurface fluorescence maximum. On August 23 and 25 the subsurface fluorescence maximum adjacent to the iceberg (station W01) was at ca. 18 m depth and on August 11, 28 and 29 the subsurface fluorescence maximum was at ca. 25 m depth (Figure 4.13).

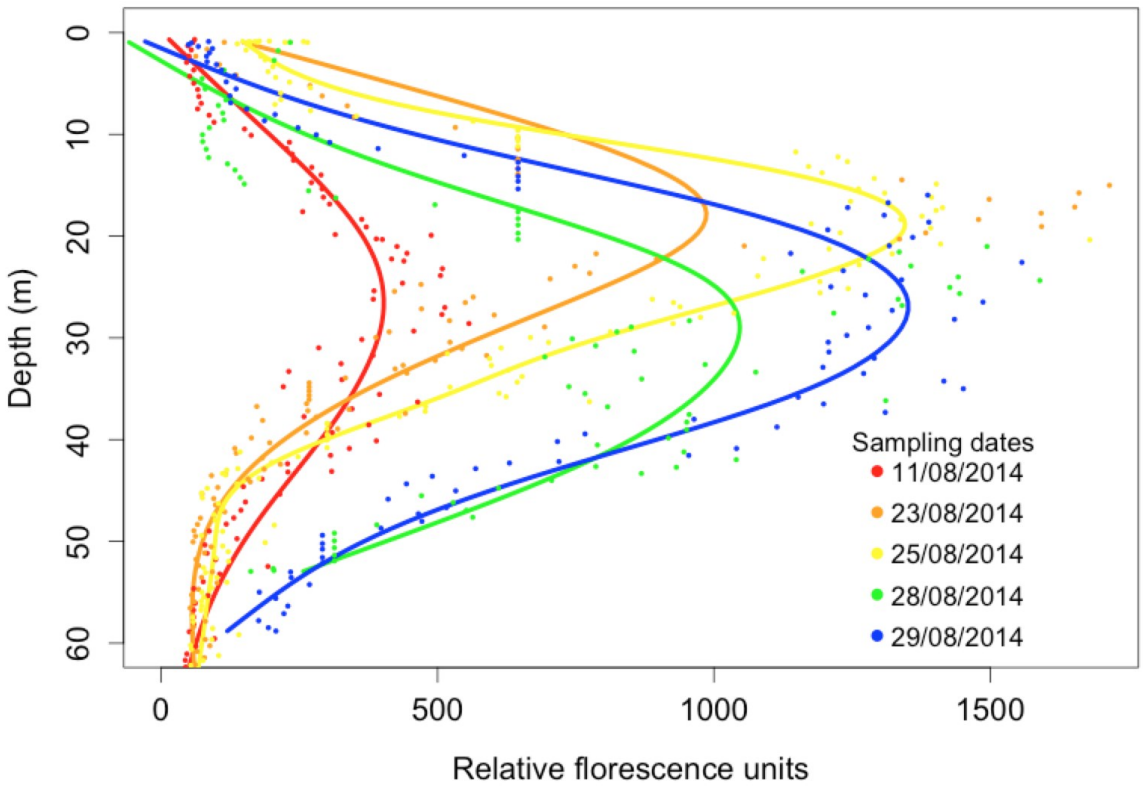


**Figure 4.13 Chlorophyll *a* fluorescence (as relative fluorescence units) and smoothed profiles (lines) adjacent to the iceberg (station W01) on five sampling dates (dd/mm/yyyy). The spline algorithm used to generate the curve may underestimate the magnitude of the chlorophyll *a* maximum.**

$NO_3^-$ and $Si(OH)_4$ concentrations in the iceberg itself were below the detection limit while $PO_4^{3-}$, DOC, total protists, picoeukaryotes, and nanoeukaryotes were very low compared to the water column (Table 4.4). Salinity ($t = 5.520$, $p < 0.001$) as well as $Chl_{TOT}$ ($t = 2.661$, $p < 0.001$) and $Chl_{5\ \mu m}$ ($t = 2.944$, $p < 0.001$) concentrations were significantly higher in the lower water column compared to the upper water column. Otherwise, DOC concentration ($t = -1.483$, $p > 0.05$), counts of total protists ($W = 114$, $p > 0.05$), picoeukaryotes ($W = 162$, $p > 0.05$), and nanoeukaryotes ($W = 114$, $p > 0.05$) were not significantly different in the lower water column compared to the upper water column.

**Table 4.3 Mean ($\bar{x}$), standard deviation (sd) and sample size (n) of nutrient concentrations ($NO_3^-$, $Si(OH)_4$, $PO_4^{3-}$), dissolved organic carbon (DOC), cell counts (total protists, picoeukaryotes, nanoeukaryotes), chlorophyll *a* total ($Chl_{TOT}$) and chlorophyll *a* > 5 µm ($Chl_{5\ \mu m}$) in the iceberg and upper and lower water column. na indicates that no samples were collected and bd indicates that the mean was below the detection limit. Bold indicates that the lower water column mean value is significantly higher than that in the upper water column**

| Variable | Iceberg | | | Upper | | | Lower | | |
|---|---|---|---|---|---|---|---|---|---|
| | $\bar{x}$ | sd | n | $\bar{x}$ | sd | n | $\bar{x}$ | sd | n |
| Nutrients | | | | | | | | | |
| $NO_3^-$ (µmol $L^{-1}$) | bd | na | 2 | bd | na | 15 | **4.77** | **4.64** | 15 |
| $Si(OH)_4$ (µmol $L^{-1}$) | bd | na | 2 | **0.89** | **0.55** | 16 | **10.19** | **9.13** | 15 |
| $PO_4^{3-}$ (µmol $L^{-1}$) | 0.02 | 0.01 | 2 | **0.47** | **0.05** | 16 | **0.96** | **0.36** | 15 |
| DOC (µmol $L^{-1}$) | 34.3 | 19.9 | 2 | **81.7** | **10.3** | 15 | **76.6** | **6.4** | 15 |
| Salinity | 0 | 0 | 6 | **29.1** | **0.9** | 34 | **31.5** | **1.3** | 13 |
| $\delta^{18}O$ (‰) | -31.38 | 0.75 | 6 | **-2.44** | **0.34** | 34 | **-1.88** | **0.46** | 13 |
| Cell counts ($10^3$ cells $mL^{-1}$) | | | | | | | | | |
| Total protists | 0.517 | 0.148 | 2 | 3.56 | 2.42 | 17 | 2.94 | 2.27 | 15 |
| Picoeukaryotes | 0.0800 | 0.0190 | 2 | 0.494 | 0.342 | 17 | 0.705 | 0.616 | 15 |
| Nanoeukaryotes | 0.432 | 0.163 | 2 | 3.01 | 2.24 | 17 | 2.22 | 1.67 | 15 |
| Chl *a* (mg $m^{-3}$) | | | | | | | | | |
| $Chl_{TOT}$ | na | na | na | 4.51 | **2.81** | **17** | **10.86** | **8** | 12 |
| $Chl_{5\ \mu m}$ | na | na | na | 3.15 | **1.88** | **17** | **8.80** | **6.61** | 12 |

# 5 Chapter: Discussion

## 5.1 Iceberg influence on water column structure

### 5.1.1 Contribution of surface freshwater

It has been suggested that the presence of an iceberg could cause density anomalies in the adjacent water column and contribute to a relatively fresh meltwater plume at the surface or at layers within the water column (Donaldson 1978; Huppert and Turner 1980). Here, $\delta^{18}O$ and salinity were used to evaluate the contribution of iceberg meltwater in the water column surrounding the iceberg, and also determine the influence of sea ice meltwater in the same region. The slope of the salinity and $\delta^{18}O$ dilution line in the upper water column (Figure 4.3) as well as the minimal contribution of iceberg meltwater (<5%) in the surface waters (Figure 4.4) indicates a notable contribution from sea ice meltwater (<18%). Due to the time of year and the warm temperatures, there was extensive sea ice meltwater in the study area while the contribution of iceberg meltwater was marginal. Other potential end-members, aside from the three identified, such as riverine input, were not considered and might have affected the results of the mixing model and the fraction of iceberg meltwater. Using average $\delta^{18}O$ measurements from six large Arctic rivers, a typical river runoff end member would be very negative (-20‰) and fresh (salinity = 0) (Cooper et al 2005). Therefore, riverine input would inflate the fraction of iceberg meltwater. However, there were no major rivers near the study area, therefore riverine input likely did not have a large effect on the results of the mixing model.

In this study, the upper water column was more depleted ($\delta^{18}O$ = -2.44‰) compared to the lower water column (-1.88‰) (Table 4.4). The significantly greater driving

temperature in the upper water column compared to the lower water column (Figure 4.10b) indicates that there is more potential for iceberg melting in the upper water column, assuming other conditions (currents and roughness) are constant. Kumiko and Francis (1997) observed a similar increase in $\delta^{18}O$ and salinity with depth by using a comparable method for analyzing glacier meltwater in an east Greenland fjord. There, $\delta^{18}O$ in the surface waters measured -5.6‰ at the head of the fjord and increased with depth until reaching a constant value of 0‰ at 200 m. In Kongsfjorden, on the west coast of Svalbard, glacial meltwater was primarily observed in the upper 15 m of the water column (Maclachlan et al. 2007). The surface waters (<2 m) and deeper waters (>2 m) had $\delta^{18}O$ measurements ranging from -1.00 to -1.47‰ and -0.02 to 0.21‰, respectively. The difference between the $\delta^{18}O$ measurements surrounding the iceberg in this study compared to those of previous studies could be due to the $\delta^{18}O$ signature of the glacial meltwater. For example, the glacier in Kongsfjorden had a $\delta^{18}O$ measurement of -15.58‰ whereas the iceberg in this study was more depleted (-31.38‰).

During this study, a significant change in $\delta^{18}O$ with distance from the iceberg was not noted; contrasting with observations in a Greenland fjord, where surface water $\delta^{18}O$ values increased with distance from the tidewater glacier (Kumiko and Francis 1997). The relatively abundant meltwater in an enclosed fjord produced a strong meltwater signal contrasting with the current study where tidal mixing, wind and surface currents would have contributed to a more homogeneous distribution of iceberg meltwater in the water column. A previous study in the Weddell Sea east of the Antarctic Peninsula showed that iceberg meltwater rises from the keel in a buoyant plume forming a relatively thin surface freshwater layer (Stephenson et al. 2011). However, the results

suggest that surface meltwater plumes are highly variable spatially, with only half of the stations within 2 km of the iceberg showing evidence of meltwater at the surface. This is underscored by a low fraction of meltwater (~0.12%) found in the surface waters in a Greenlandic fiord with a large subglacial discharge of freshwater (C. Richards, pers. comm.). This phenomenon is likely due to the iceberg meltwater not rising all the way to the surface, but instead finding a neutrally buoyant level in the water column (Stephenson et al. 2011).

### 5.1.2 Mixing and upwelling

The temperature and salinity profiles observed in the study area were typical of Arctic summer conditions, where warmer fresh surface waters and a steep pycnocline at an average depth of 18.5 m (Figures 4.6 to 4.10) are the result of solar heating and freshwater fluxes from sea ice meltwater and, in localized areas, from river runoff (Carmack et al 2016). However, the water column structure within 30 m of the iceberg was unique; with colder and more saline surface waters to the east, west and north sides of the iceberg. The pycnocline was not significantly deeper adjacent to the iceberg compared to all other stations, however, this may be due to the variability in pycnocline depth at all the stations not adjacent to the iceberg and lack of statistical power. The colder and more saline surface waters indicate mixing between the surface and deeper waters and possibly upwelling of colder saline waters in the very close vicinity of the iceberg. These mixing and upwelling processes likely result from the topographic influence of the iceberg on currents (e.g., Grosfeld et al. 2001; Robinson et al. 2010).

Icebergs can influence local water currents through a variety of processes. Grounded icebergs can act in a similar fashion to islands (Send et al. 1987), where depending on the

angle between currents and the sides of the icebergs, eddies can be created, resulting in mixing and upwelling (Hamner and Haurl 1981). Alternatively, the shape of the iceberg below the water surface could be irregular, causing deflected water to upwell.

With buoyant convection, water will only rise or fall until it reaches the level of neutral density (Huppert and Turner 1980). At that point, the water commences to move horizontally, forming a series of layers adjacent to the iceberg, where a relatively thin layer of ambient seawater separates each layer, resulting in double-diffusive processes. According to equation 3.2, isopycnal water layers of 0.1 to 0.5 m are expected to occur near an iceberg in water conditions representative of local far-field conditions at the study site (station S08; Figure 4.10c). The fact that observed thermohaline steps in the profiles adjacent to the iceberg were two orders of magnitude higher, indicates that any steps created by rising iceberg meltwater were merged together or greatly enhanced by turbulence from currents and wind (Jacobs et al. 1981; Stephenson et al. 2011). Stephenson et al. (2011) determined that in waters less than 50 m depth, the air-sea heat flux and winds caused mixing near an Antarctic iceberg and diminished any stratified step structure in the upper mixed layer, whereas the observed and predicted layer thickness matched better in deeper waters. The thicknesses of the predicted isopycnal layers in this study (0.1 to 0.5 m) were an order of magnitude smaller than those of observed (2.5 to 50 m) <2 km from an iceberg in the Weddell Sea (Stephenson et al. 2011). This is probably due to the much smaller far-field density gradient ($d\rho/dz$ in eqn. 3.2) in those Antarctic waters. The lower bound of observed isopycnal layers observed by Jacobs et al. (1981) adjacent to the Erebus Glacier Tongue (7 to >50 m) are more similar to those observed in the present study (6.3 to 40 m), in spite of a similarly large

far-field density gradient difference. Predicted isopycnal layer thickness from equation 3.2 is very sensitive to the computation of the far-field gradient from two depths in the profile. As well, Huppert and Turner (1980) derived their formula under a constant gradient, which is not the case at station S08 from 5 to 50 m depth (Figure 4.10). Therefore, this may explain some of the discrepancy between observed and predicted layer thickness (*cf*. Stephenson et al. 2011) but this does not contradict the interpretation that other causes of mixing are far more important than meltwater from buoyant convection in this environment.

Some studies have demonstrated double-diffusive processes in ocean waters adjacent to melting icebergs (Stephenson et al. 2011; Huppert and Turner 1980; Jacobs et al. 1981). The thermohaline staircases observed in this study do not show small, regular steps with a systematic offset between salinity and temperature which suggests that double-diffusion was not occurring. This is likely due to the high degree of turbulence from tidal currents (Cota et al. 1987) and wind (Figure 3.1).

In addition to mixing and upwelling processes, the disparities in temperature and salinity characteristics on different sides on a grounded iceberg may be due to dominant winds giving rise to Ekman transport. Stern et al. (2015) determined that wind-driven Ekman transport caused upwelling of cold, saline water on the side of the ice island that was to the right of the wind direction and downwelling of warm and fresh surface water on the opposite side creating a pronounced thermocline. In this study, cold and saline surface waters as well as a deep pycnocline were observed on both the upwind and downwind sides of the relatively small iceberg, therefore, wind induced Ekman transport was likely not a factor in this case. During the three days prior to sampling on August

11th, the wind direction was fairly consistent and it is likely that the strong currents in the study area had a larger influence than wind direction on mixing processes near the iceberg.

The direction of the surface water currents near the iceberg was noted during the collection of water samples on August 11th. Using this anecdotal evidence, a schematic of the possible flow of water around the iceberg at the surface was sketched in Figure 5.1 to explore conceptually how the currents might have influenced the upper water column profiles adjacent to the iceberg at that point in time. At the upstream (north and west) stations the surface water currents flowed towards the iceberg while at the eastern station the surface waters flowed in the southeast direction. The direction of the surface water currents and the interference with the iceberg at the north, west, and east stations likely caused mixing and possibly upwelling. At the southern station the surface water currents flowed parallel to the iceberg, in the eastward direction, therefore the presence of the iceberg may not have influenced the surface water currents. Due to the slope of the iceberg sail, surface meltwater was flowing off the iceberg in the vicinity of the southern station, which resulted in a fresh and stratified upper 10 m depth.

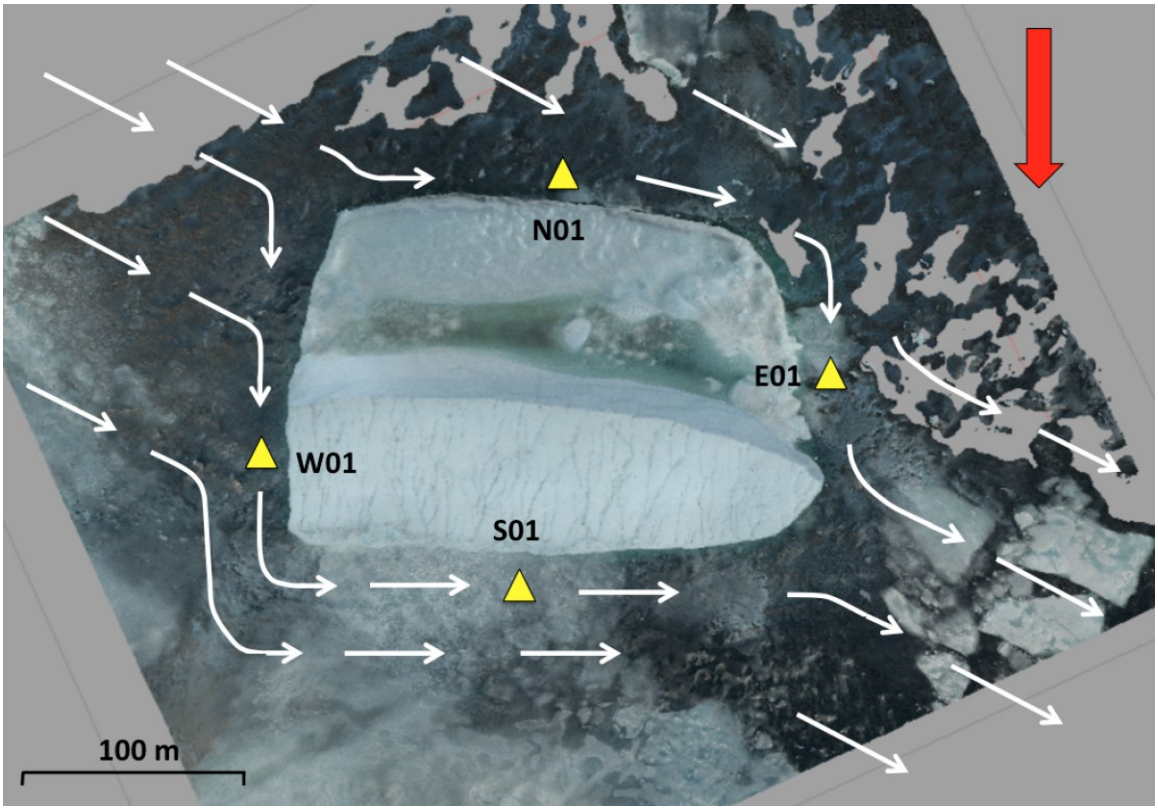


**Figure 5.1 Schematic of the possible flow of water (white arrows) around the iceberg on August 11th, 2014 with stations N01, E01, S01 and W01 marked with yellow triangles. Wind direction (red arrow) was northerly. The beige areas in the water are artefacts from photo mosaicking.**

## 5.2 Stratification and nutrient limitation

During the sampling period the surface waters were strongly stratified, with a steep pycnocline at an average depth of 18.5 m, ranging from 7 and 30 m depth (Figures 4.6 to 4.10). Ardyna et al. (2011) recorded similar pycnocline depths in the CAA in fall 2006 and 2007, with average pycnocline depths of 10 and 19 m, respectively. Similar to previous studies, the stratification of the water column was primarily caused by sea ice melt and potential riverine input (Behrenfeld et al. 2006; Carmack and Wassmann 2006; Carmack 2007; Yamamoto-Kawai et al. 2009). The low nutrient concentrations above the pycnocline (Table 4.4.) were likely the result of phytoplankton uptake (e.g., Ardyna et al. 2011). The strongly stratified water column limited vertical water movement, thus

prohibiting the replenishment of the nutrients in the upper water column from below. Nutrient depletion in the upper water column was evident on August 11$^{th}$, which was only three days after the sea ice cover decreased from >50% to 0% (Figure 4.2). This indicates that a phytoplankton bloom began prior to sea ice break-up. As demonstrated by Fortier et al. (2002), the minimal snow and fragmented condition of the sea ice likely allowed increased sunlight to reach the water, thus stimulating productivity. Similar nutrient depletion in the upper 30 m of the water column and an under-ice phytoplankton bloom was observed on the Chukchi Sea continental shelf at the beginning of July (Arrigo et al. 2012).

Despite the large variation in the nitrogen to phosphorus ratios within phytoplankton (Arrigo et al. 1999), Redfield ratios are useful to identify limiting nutrients for primary production. While $NO_3^-$ was depleted in the upper water column, $Si(OH)_4$ concentrations were low but not depleted (Figure 4.12 and Table 4.4). Therefore, similar to recent studies in the Arctic (Tremblay et al. 2002, 2006, 2008; Walsh et al. 2004; Rozanska et al. 2009), nitrogen was identified as the growth-limiting nutrient.

The high $NO_3^-$ concentrations in the lower water column (4.77 μmol $L^{-1}$) compared to the upper water column (<0.051 μmol $L^{-1}$) (Table 4.4) are comparable to those in previous studies. In Jones Sound, $NO_3^-$ concentrations in the upper waters were undetectable in the late summer and fall (Apollonio and Matrai 2011; Platt et al. 1987). $PO_4^{3-}$ concentrations in the upper (0.470 μmol $L^{-1}$) and lower (0.958 μmol $L^{-1}$) water column observed in this study were similar to concentrations at the pycnocline in the Canadian Arctic Archipelago in the summer of 2005 (1.00 μmol $L^{-1}$) and in early fall of 2006 (0.92 μmol $L^{-1}$) (Ardyna et al. 2011). Ardnya et al. (2011) observed decreased

$Si(OH)_4$ concentrations compared to the upper (0.89 μmol $L^{-1}$) and lower water column (10.19 μmol $L^{-1}$) in this study. However, Michel et al. (2006) recorded higher average $Si(OH)_4$ concentrations of 6.21 μmol $L^{-1}$ and 25.09 μmol $L^{-1}$ in the upper (<25 m) and lower (>25 m) water column, respectively, in Barrow Strait during August. Overall, $NO_3^-$, $PO_4^{3-}$, and $Si(OH)_4$ were comparable to previous measurements.

Iceberg meltwater in the Antarctic is a source of iron, a limiting nutrient for primary production, and can thereby create productive regions in their wake (Smith et al. 2007; Duprat et al. 2016). In this study, as in other areas of the Arctic (e.g., Tremblay et al. 2008; Walsh et al. 2004; Rozanska et al. 2009), nitrogenous nutrients are considered to be limiting for primary production. The extremely low ($PO_4^{3-}$) and below detection ($NO_3^-$, $Si(OH)_4$) nutrient concentrations measured in the iceberg meltwater clarify that the iceberg is not a source of nutrients to the surface waters in this study (Table 4.3). The iceberg was also not a significant source of protists, pico- and nanoeukaryotes or DOC.

The physical structure of the water column in close proximity to the iceberg (30 m) and the associated mixing processes described in the previous section suggest that upwelling may occur near the iceberg. However, our small sample size was insufficient to document any increase in surface nutrient concentrations near the iceberg, compared to 8 km offshore ($NO_3^-$ was below detection at Station S11). Furthermore, there was no evidence for upwelling of bottom water to the surface since a pycnocline separating the upper and lower water column persisted throughout the sampling period. It was concluded that the regional nutrient dynamics in the study area were determined by the strong pycnocline and the early drawdown by phytoplankton, whereas the iceberg could have contributed very locally to mixing events. The influence of this local mixing on

nutrient replenishment in the surface layer is anticipated to depend on the size and shape of icebergs, as well as on their location and interaction with physical factors including circulation patterns and the direction and persistence of wind events.

### 5.3 Early phytoplankton bloom development

The very high chl *a* concentrations observed during this study, with average maximum subsurface chl *a* concentrations of 17.9 mg $m^{-3}$ and average integrated concentrations of 570 mg $m^{-2}$. The high proportion of chl *a* to total pigment (mean: 0.93, std: 0.1) indicates the presence of fresh algal material rather than degraded algae. These concentrations are in the higher range of chl *a* concentrations measured on Arctic shelves and are comparable with productive regions, such as the Cape Bathurst polynya, located in the Amundsen Gulf (Arrigo and Van Dijken 2004). In May 1988, certain locations within the Cape Bathurst polynya had chl *a* concentrations exceeding 20 mg $m^{-3}$. Chl *a* concentrations greater than 20 mg $m^{-3}$ were similarly observed during a bloom in Barrow Strait at the end of July–early August in the upper 10–15 m of the water column (Michel et al. 2006). While the chl *a* concentrations in this study are comparable to productive regions, the measurements typically exceed those of other studies in the area. For example, in 1956, Apollonio and Matrai (2011) recorded maximum chl *a* measurements of 5.5 mg $m^{-3}$ in Allen Bay shortly after the break up of the sea ice in mid-July. The average integrated phytoplankton biomass in the Canadian Arctic Archipelago in late summer of 2005 (38.3 mg $m^{-2}$) and early fall of 2006 (22.6 mg $m^{-2}$) (Ardyna et al. 2011) were much lower than the measurements in this study. The integrated chl *a* measurements in this study were comparable to typical values observed by Michel et al. (2006) in Barrow Strait at the end of July–early August, with maximum chl *a* biomass of 540 mg

$m^{-2}$ (for the 0–30 m depth interval) in the upper 10–15 m of the water column.

In previous studies, the stratification of the water column limited the vertical movement of nutrients causing a deepening of the chl *a* maximum down to the nutricline (Kattner and Becker 1991; Gradinger and Baumann 1991) and a concomitant shift in photo-acclimatization in the algae to compensate for lower light levels (Tremblay et al. 2002). A similar deepening and strengthening of the chl *a* maximum may have occurred in this study. The repeated sampling at station W01 (Figure 4.13) shows a deepening of the chl *a* maximum from ca. 15 to ca. 25 m between August 23 to 28, however, a more extensive spatial and temporal sampling prior to and during the period of ice melt is required to fully support this conclusion.

Nutrient depletion in the upper water column in combination with the high chl *a* concentrations (Table 4.4) suggests that the phytoplankton bloom was ongoing or had just terminated during the study. The timing of the bloom compares well to a compilation of 11 years of data collected in the Barrow Strait, which shows that the summer bloom typically develops at the time of sea ice break up during the month of July and peaks at the end of July or early August (Michel et al. 2006). This average timing is slightly earlier than what was found in this study, although the results are within the typical interannual variability (Michel et al. 2006, Apollonio and Matrai 2011).

In general terms, phytoplankton regimes can be classified as either a diatom or flagellate-based system (Cushing 1989), both of which are found in the Arctic (e.g., Li et al. 2009, Tremblay et al. 2009). The high chl *a* concentrations, and higher abundance of nanoeukaryotes compared to picoeukaryotes (Table 4.3) support the dominance of a diatom-based system. This is further confirmed by the $Si(OH)_4$ depletion in the upper

water column (0.89 μmol $L^{-1}$ versus 25.66 μmol $L^{-1}$ at 110 m at S11). Diatom-based phytoplankton communities have also been observed in different well-mixed euphotic waters in Baffin Bay, Lancaster Sound, and the Amundsen Gulf hotspot during late summer 2005 and fall 2007 (Ardyna et al. 2011). In contrast, flagellates-based systems have been observed in stratified environments, such as the Beaufort Sea and central region of the CAA (Ardyna et al. 2011; Carmack et al. 2004; Simpson et al. 2008; Tremblay et al. 2009). The stratification of the water column in the study area suggests that the system would eventually switch to a flagellate-based system.

### 5.4 Significance

There is currently scientific debate and uncertainty regarding the biogeochemical response of the world's oceans to climate change (Boyce et al. 2010; Behrenfeld 2011; Chavez et al. 2011; Steinacher et al. 2010; Taucher and Oschlies 2011). Remote sensing studies suggest that a global decrease in oceanic phytoplankton biomass has occurred over the past century (Boyce et al. 2010, 2011) as the result of reduced nutrient input into the euphotic zone from enhanced stratification (Steinacher et al. 2010). Additionally, an increase in the frequency and intensity of storms at high latitudes (McCabe et al. 2001; Zhang et al. 2004; Yang 2009) suggests that vertical mixing events and the replenishment of nutrients into the photic zone will be more frequent in the future. Arctic phytoplankton production, estimated from remote sensing, has been shown to increase by 30% between 1998 and 2009 in the Arctic Ocean due to decreasing sea ice extent (Arrigo and Dijken 2015). Chavez et al. (2011) suggest that global marine primary production has increased from 1950 to present due to upper water column warming, which can stimulate plankton metabolism and enhance photosynthesis.

Under-ice phytoplankton blooms are possibly more widespread than previously thought (Arrigo et al. 2012; Fortier et al. 2002; Mundy et al. 2009). The results from this study, as well as previous studies on Arctic shelves (Matrai and Apollonio, 2013; Michel et al. 2015), suggest that current primary production on Arctic continental shelves is likely underestimated. In order to understand the impacts of future climate-associated changes in the Arctic marine environment more research is needed to determine the magnitude and spatial distribution of phytoplankton blooms in open water and under sea ice on Arctic shelves.

Studies concerning the impacts of icebergs on the surrounding marine environment in the Canadian Arctic are rare. While the iceberg in this study was not observed to directly influence phytoplankton biomass or nutrient dynamics, further studies are needed to evaluate the potential influence of icebergs on longer time scales and under different circulation regimes. This study was conducted during extensive sea ice melt and strong water column stratification; it is possible that the influence of high tides and strong water currents could have diminished the detectability and importance of iceberg meltwater. Changes in biological activity surrounding Canadian icebergs might be observed near larger icebergs, with more meltwater, or in areas with small water currents.

Furthermore, the frequency of ice shelf and floating glacier tongue calving events is predicted to increase due to recent Arctic climate change (Peterson 2005; Copland et al. 2007). These icebergs could modify local mixing events on Arctic shelves, through the injection of meltwater and by altering water circulation patterns. These mixing events

could influence nutrient replenishment in the upper water column and could be associated with increased biological activity, although this was not evident in the current study.

# 6 Chapter: Conclusion

The objectives of this study were to determine the contribution and extent of the iceberg meltwater and its influence on water column structure as well as evaluate the influence of an iceberg on phytoplankton biomass and nutrient dynamics. The results of the mixing model indicate that iceberg meltwater was significantly higher in the upper water column compared to the lower water column. However, the iceberg had only a small contribution on surface meltwater while sea ice meltwater had a relatively larger influence. The fraction of iceberg meltwater was not significantly higher directly adjacent to the iceberg compared to all other stations. This was likely due to the relatively large tides and water currents, which could have quickly dispersed the meltwater. This result is further corroborated by the larger than expected steps in density adjacent to the iceberg. Iceberg meltwater may have contributed to these profiles but was likely overshadowed by other processes such as mixing by wind and tidal currents.

Over the study area, the water column was characterized by warmer fresh surface waters and a strong pycnocline. As in other studies, stratification likely formed primarily due to sea ice meltwater (Aagaard et al. 1981; Anderson et al. 2013; Ferguson et al. 2010). Adjacent to the iceberg, the surface waters were colder and more saline, suggesting that the iceberg either cooled the surrounding water and/or may have been responsible for the upward advection of relatively cold, saline water from depth. However, the pycnocline was not significantly deeper adjacent to the iceberg compared to all other stations, which may reflect the variability in pycnocline depth at all the stations not adjacent to the iceberg and/or statistical limitations due to small sample size. The changes to the physical structure of the water column adjacent to the iceberg were

likely due to the interference of the iceberg with the surrounding ocean currents rather than from iceberg meltwater. The impact of an iceberg to the water column structure could depend on the size and shape of the iceberg, as well physical factors, such as water currents and the direction and persistence of wind events. Further studies are needed concerning the impacts of icebergs on the physical structure of the water column. Ideally these studies would occur on longer time scales and under different water circulation regimes.

Phytoplankton biomass and nutrient concentrations were not significantly higher directly adjacent to the iceberg compared to all other stations. Therefore, the iceberg did not impact regional nutrient dynamics, however, due to the small sample size as well as temporal and spatial limitations, further studies are needed. Ideally, these studies would take place during the summer months, when the maximum amount of melt is occurring, and in an area with relatively low water currents in order to observe the direct effects of iceberg meltwater in causing density anomalies.

The high chl *a* measurements were observed in this study and are comparable to other productive regions in the Arctic, such as the Cape Bathurst polynya (Arrigo and Van Dijken 2004). These chl *a* measurements, as well as the low $NO_3^-$ concentrations in the upper water column, suggested that a phytoplankton bloom was ongoing and likely began before the break up of the sea ice. Similar to other studies, the stratification of the water column limited the vertical movement of the nutrients, causing the subsurface chl *a* maximum to deepen to the nutricline over the sampling period (Kattner and Becker 1991; Gradinger and Baumann 1991). Large phytoplankton cells (>5 μm) dominated the bloom, indicating the presence of a diatom-based community. The magnitude and timing of the

phytoplankton bloom observed in this study indicate that primary production on Arctic continental shelves may be drastically underestimated. Further research concerning phytoplankton bloom dynamics in open water and under sea ice on Arctic shelves is needed. This is of particular importance in order to understand and predict the impacts of ongoing and future climate change on the Arctic marine environment.

## References


AMAP. 2011. "SWIPA: Snow, Water, Ice and Permafrost in the Arctic. Arctic Monitoring and Assessment Programme (AMAP)." Oslo, Norway. pp. 20-23.

Anderson, L.G., G. Bjrrk, E.P. Jones, G. Kattner, K.P. Koltermann, B. Liljeblad, R. Lindegren, B. Rudels, and J. Swift. 1994. "Water masses and circulation in the Eurasian Basin: Results from the Oden 91 Expedition." *J. Geophys. Res.* 99: 3273–83.

Anderson, L.G., P.S. Andersson, G. Björk, E.P. Jones, S. Jutterström, and I. Wåhlström. 2013. "Source and formation of the upper halocline of the Arctic Ocean." *J. Geophys. Res. Oceans* 118: 410–21. doi:10.1029/2012JC008291.

Apollonio, S., and P. Matrai. 2011. "Marine primary production in the Canadian Arctic, 1956, 1961 – 1963." *Polar Biol.* 34: 767–74. doi:10.1007/s00300-010-0928-3.

Ardyna, M., M. Gosselin, C. Michel, M. Poulin, and J.-É. Tremblay. 2011. "Environmental forcing of phytoplankton community structure and function in the Canadian High Arctic: Contrasting oligotrophic and eutrophic regions." *Mar. Ecol. Prog. Ser.* 442: 37–57. doi:10.3354/meps09378.

Arrigo, K.R., D.H. Robinson, D.L. Worthen, R.B. Dunbar, G.R. DiTullio, M. VanWoert, and M.P. Lizotte. 1999. "Phytoplankton community structure and the drawdown of nutrients and $CO_2$ in the Southern Ocean." *Science* 283: 365–67.

Arrigo, K.R., and G.L. Van Dijken. 2015. "Increases in Arctic Ocean primary production." *Prog. Oceanogr.* 136: 60–70. doi:10.1016/j.pocean.2015.05.002.

Arrigo, K.R., G.L. Van Dijken, D.G. Ainley, M.A. Fahnestock, and T. Markus. 2002. "Ecological impact of a large Antarctic iceberg" *Geophys. Res. Lett.* 29 (7): 6–9.

Arrigo, K.R., D.K. Perovich, R.S. Pickart, Z.W. Brown, G.L. Van Dijken, K.E. Lowry, M.M. Mills, M.A. Palmer, W.M. Balch, F. Bahr, N.R. Bates, C. Benitez-Nelson, B. Bowler, E. Brownlee,J.K. Ehn, K.E. Frey, R. Garley, S.R. Laney, L. Lubelczyk,J. Mathis, A. Matsuoka, B.G. Mitchell, G.W.K. Moore, E. Ortega-Retuerta, S. Pal, C.M. Polashenski, R.A. Reynolds, B. Schieber, H.M. Sosik, M. Stephens, J.H. Swift. 2012. "Massive phytoplankton blooms under Arctic sea ice." *Science* 336: 1408. doi:10.1126/science.1215065.

Arrigo, K.R., and G.L. Van Dijken. 2004. "Annual cycles of sea ice and phytoplankton in Cape Bathurst polynya, Southeastern Beaufort Sea, Canadian Arctic." *Geophys. Res. Lett.* 31 (L08304). doi:10.1029/2003GL018978.

Ballicater Consuting Ltd. 2012. "Ice Island and Iceberg Studies 2012." Report prepared for the Canadian Ice Service, Environment Canada, Ottawa. Report 12-01, pp. 51

Behrenfeld, M.J., R.T. O'Malley, D.A. Siegel, C.R. McClain, J.L. Sarmiento, G.C. Feldman, A.J. Milligan, P.J. Falkowski, R.M. Letelier, and E.S. Boss. 2006. "Climate-driven trends in contemporary ocean productivity." *Nature* 444: 752−755.

Behrenfeld, M. 2011. "Uncertain future for ocean algae." *Nature Clim. Change* 1: 33–34. doi:10.1038/nclimate1069.

Belzile, C., S. Brugel, C. Nozais, Y. Gratton, and S. Demers. 2008. "Variations of the abundance and nucleic acid content of heterotrophic bacteria in Beaufort Shelf waters during winter and spring." *J. Mar. Res.* 74 (3-4): 946–56. doi:10.1016/j.jmarsys.2007.12.010.

Bergmann, M.A., H.E. Welch, J.E. Butler-Walker, and T.D. Siferd. 1991. "Ice algal photosynthesis at Resolute and Saqvaqjuac in the Canadian Arctic." *J. Marine Syst.* 2 (1): 43–52.

Berman, E.S.F., N.E. Levin, A. Landais, S. Li, and T. Owano. 2013. "Measurement of $\delta^{18}O$, $\delta^{17}O$, and $^{17}O$-excess in water by off-axis integrated cavity output spectroscopy and isotope ratio mass spectrometry." *Anal. Chem.* 85: 10392–98.

Boyce, D.G., M.R. Lewis, and B. Worm. 2011. "Is there a decline in marine phytoplankton? Boyce et al. reply." *Nature* 472: E8−E9.

Boyce, D.G., M.R. Lewis, and B. Worm. 2010. "Global phytoplankton decline over the past century." *Nature* 466 (7306): 591–96. doi:10.1038/nature09268.

Brown, Z.W., K.E. Lowry, M.A. Palmer, G.L. Van Dijken, M.M. Mills, R.S. Pickart, and K.R. Arrigo. 2015. "Characterizing the subsurface chlorophyll *a* maximum in the Chukchi Sea and Canada Basin." *Deep-Sea Res. Pt II* 118: 88–104. doi:10.1016/j.dsr2.2015.02.010.

Carmack, E. 2007. "The alpha / beta ocean distinction: A perspective on freshwater fluxes, convection, nutrients and productivity in high-latitude seas." *Deep-Sea Res. Pt II* 54: 2578–98. doi:10.1016/j.dsr2.2007.08.018.

Carmack, E.C., R.W. Macdonald, and S. Jasper. 2004. "Phytoplankton productivity on the Canadian Shelf of the Beaufort Sea." *Mar. Ecol. Prog. Ser.* 277: 37–50.

Carmack, E., and P. Wassmann. 2006. "Food webs and physical – biological coupling on pan-Arctic shelves: Unifying concepts and comprehensive perspectives." *Prog. Oceanogr.* 71: 446–77. doi:10.1016/j.pocean.2006.10.004.

Carmack, E. C., M. Yamamoto-Kawai, T.W.N. Haine, S. Bacon, B.A. Bluhm, C. Lique, H. Melling, I.V. Polyakov, F. Strameo, M.-L. Timmermans, and W.J. Williams. 2016. "Freshwater and its role in the Arctic marine system: Sources, disposition, storage, export, and physical and biogeochemical consequences in the Arctic and

global oceans." *J. Geophys. Res. Biogeosci.* 121: 675–717, doi:10.1002/2015JG003140.

Cefarelli, A.O., M. Vernet, and M.E. Ferrario. 2011. "Phytoplankton composition and abundance in relation to free-floating Antarctic icebergs." *Deep-Sea Res. Pt II* 58: 1436–50. doi:10.1016/j.dsr2.2010.11.023.

Chavez, F.P., M. Messi, and J.T. Pennington. 2011. "Marine primary production in relation to climate variability and change." *Ann. Rev. Mar. Sci.* 3: 227-60. doi:10.1146/annurev.marine.010908.163917.

Chester, R. 2003. Marine Geochemistry, Second Ed. Blackwell Publishing, pp. 506.

Cohen, J., J.A. Screen, J.C. Furtado, M. Barlow, D. Whittleston, D. Coumou, J. Francis, K. Dethloff, D. Entekhabi, J. Overland and J. Jones. 2014. "Recent Arctic amplification and extreme mid-latitude weather." *Nat Geosci.* 7: 627-637. doi:10.1038/ngeo2234.

Copland, L., D.R. Mueller, and L. Weir. 2007. "Rapid loss of the Ayles Ice Shelf, Ellesmere Island, Canada." *Geophys. Res. Lett.* 34: L21501 doi:10.1029/2007GL031809.

Cota, G.F., S.J. Prinsenberg, E.B. Bennett, J.W. Loder, M.R. Lewis, J.L. Anning, N.H.F. Watson, and L.R. Harris. 1987. "Nutrient fluxes during extended blooms of Arctic ice algae." *J. Geophys. Res.* 92 (C2): 1951–62.

Crawford, A. J. 2013. "Ice island deterioration in the Canadian Arctic: Rates, patterns and model evaluation." M.Sc. Thesis, Department of Geography and Environmental Studies, Carleton University, pp. 127.

Cushing, D.H. 1989. "A difference in structure between ecosystems in strongly stratified waters and in those that are only weakly stratified." *J. Plankton Res.* II (1): 1–13.

Donaldson, Peter B. 1978. "Melting of Antarctic icebergs." *Nature* 275: 305–6.

Duprat, L.P.A.M, R.B. Grant, and D.J. Wilton. 2016. "Enhanced Southern Ocean marine productivity due to fertilization by giant icebergs." *Nat. Geosci.* 9: 219–21. doi:10.1038/ngeo2633.

Fenchel, T. 1988. "Marine plankton food chains." *Ann. Rev. of Ecol. and Syst.* 19: 19–38.

Fofonoff, N.P., and R.C. Millard. 1991. Calculation of Physical Properties of Seawater. WOCE Operations Manual, T. Joyce, Editor, WOCE Hydrographic Programme Office, WHPO, 91-1.

Fortier, M., L. Fortier, C. Michel, and L. Legendre. 2002. "Climatic and biological forcing of the vertical flux of biogenic particles under seasonal Arctic sea ice." *Mar. Ecol. Prog. Ser.* 225: 1–16.

Garneau, M-E., M. Gosselin, B. Klein, J- É. Tremblay, and E. Fouilland. 2007. "New and regenerated production during a late summer bloom in an Arctic polynya." *Mar. Ecol. Prog. Ser.* 345: 13–26. doi:10.3354/meps06965.

Garrett, C., and E. Horne. 1978. "Frontal circulation due to cabbelling and double diffusion." *J. Geophys. Res.* 83: C9.

Gosselin, M., L. Legendre, S. Demers, and R.G. Ingram. 1985. "Responses of sea-ice microalgae to climatic and fortnightly tidal energy inputs (Manitounuk Sound, Hudson Bay)." *Can. J. Fish. Aquat. Sci.* 42: 999-1006

Gradinger, R., and M.E.M. Baumann. 1991. "Distribution of phytoplankton communities in relation to the large-scale hydrological regime in the Fram Strait." *Mar. Biol.* 111: 311–21. doi:10.1007/BF01319714.

Grasshoff, K., K. Kremling, and M. Ehrhardt. 1999. Methods of Seawater Analysis, 3rd Edn. Wiley-VCH, New York. NY. pp. 632.

Grosfeld, K., M. Schrder, E. Fahrbach, R. Gerdes, and A Mackensen. 2001. "How iceberg calving and grounding change the circulation and hydrography in the Filchner Ice Shelf-ocean system." *J. Geophys. Res.* 106 (15): 9039–55.

Hamner, W.M., and I.R. Haurl. 1981. "Effects of island mass: Water flow and plankton pattern around a reef in the Great Barrier Reef Lagoon, Australia." *Limnol. Oceanogr.* 26: 1084–1102.

Helly, J.J., R.S. Kaufmann, G.R. Stephenson, and M. Vernet. 2011. "Dilution and mixing of ocean water by free-drifting icebergs in the Weddell Sea." *Deep-Sea Res. Pt II* 58 (11-12): 1346–63. doi:10.1016/j.dsr2.2010.11.010.

Horne, E.P.W. 1985. "Ice-induced vertical circulation in an Arctic fiord." *J. Geophys. Res.* 90 (20): 1078–86.

Huppert, H.E., and J.S. Turner. 1980. "Ice blocks melting into a salinity gradient." *J. Fluid Mech.* 100: 367–84. doi:10.1017/S0022112080001206.

IOC, SCOR and IAPSO. 2010. "The International Thermodynamic Equation of Seawater: Calculation and Use of Thermodynamic Properties." Intergovernmental Oceanographic Commission, Manuals and Guides No. 56, UNESCO (English), pp. 196.

Jacobs, S.S., H.E. Huppert, G. Holdsworth, and D.J. Drewry. 1981. "Thermohaline steps induced by melting of the Erebus Glacier Tongue." *J. Geophys. Res.* 86 (1): 6547–55.

Jakobsson, M., A. Grantz, Y. Kristoffersen, and R. MacNab. 2004. "Bathymetry and physiography of the Arctic Ocean and its constituent seas." In: Stein, R., Macdonald, R.A. (Eds.), The Organic Carbon Cycle in the Arctic Ocean. Springer,

Berlin, Heidelberg. pp. 1-32.

Jeffries, M.O. 1992. “Arctic ice shelves and ice islands: Origin, growth and disintegration, physical characteristics, structural-stratigraphic variability, and dynamics.” *Revi. Geophy.* 30: 245–67.

Jeffries, M.O., W.M. Sackinger, and H.D. Shoemaker. 1987. “Geometry and physical properties of ice islands.” In: 9th International Conference on Port and Ocean Engineering under Arctic Conditions. pp. 69-83.

Kattner, G., and H. Becker. 1991. “Nutrients and organic nitrogenous compounds in the marginal ice zone of the Fram Strait.” *J. Marine Syst.* 2 (3): 385–94.

Knap, A., A. Michaels, A. Close, H. Ducklow, and A. Dickson. 1996. “Protocols for the Joint Global Ocean Flux Study (JGOFS) Core Measurements”. JGOFS Report No 29. Paris: UNESCO.

Koenig, L.S., K.R. Greenaway, M. Dunbar, and G. Hattersley-Smith. 1952. “Arctic ice islands.” *Arctic* 5: 67–103.

Krajick, K. 2001. “Tracking icebergs for clues to climate change.” *Science* 292: 2244–45.

Kristensen, M. 1983. “Iceberg calving and deterioration in Antarctica.” *Prog. Phys. Geog.* 7 (3): 313-328. doi:10.1177/030913338300700301.

Kubat, I., M. Sayed, S.B. Savage, and T. Carrieres. 2005. “An operational model of iceberg drift.” *Int. J. Offshore Polar Eng.* 5(2):1–7.

Kumiko, A., and C.T. Francis. 1997. “Oxygen isotope studies from Iceland to an East Greenland Fjord : Behaviour of glacial meltwater plume.” *Mar. Chem.* 56: 239–51.

Leu, E, C.J. Mundy, P. Assmy, K. Campbell, T.M. Gabrielsen, M. Gosselin, T. Juul-Pedersen, and R. Gradinger. 2015. “Arctic spring awakening – steering principles behind the phenology of vernal ice algal blooms.” *Prog. Oceanogr.* 139: 151–70. doi:10.1016/j.pocean.2015.07.012.

Li, W.K.W., F.A. Mclaughlin, C. Lovejoy, and E.C. Carmack. 2009. “Smallest algae thrive as the Arctic Ocean freshens.” *Science* 326: 539.

Lin, H., S. Rauschenberg, C.R. Hexel, T.J. Shaw, and B.S. Twining. 2011. “Free-drifting icebergs as sources of iron to the Weddell Sea.” *Deep-Sea Res. Pt II* 58:1392–1406. doi:10.1016/j.dsr2.2010.11.020.

Long, D.G., Ballantyne, J., Bertoia, C., 2002. “Is the number of icebergs around Antarctica increasing?” *Eos, Trans. Amer. Geophys. Union.* 42: 469–474.

MacLachlan, S.E., F.R. Cottier, W.E.N. Austin, and J.A. Howe. 2007. “The Salinity: $\delta^{18}O$ water relationship in Kongsfjorden, Western Spitsbergen,” *Polar Res.* 26: 160-

167. doi:10.1111/j.1751-8369.2007.00016.x.

MANICE. 2005. Environment Canada (MANICE): Manual of Standard Procedures for Observing and Reporting Ice Conditions, Revised 9th Ed. Canadian Ice Service, Environment Canada, Ottawa, ON. pp. 146.

Martin, J., J-É. Tremblay, J. Gagnon, G. Tremblay, A. Lapoussière, C. Jose, M. Poulin, M. Gosselin, Y. Gratton, and C. Michel. 2010. "Prevalence, structure and properties of subsurface chlorophyll maxima in Canadian Arctic waters." *Mar. Ecol. Prog. Ser.* 412: 69–84. doi:10.3354/meps08666.

Martiny, A.C., J.A. Vrugt, F.W. Primeau, and M.W. Lomas. 2013. "Regional variation in the particulate organic carbon to nitrogen ratio in the Surface Ocean." *Global Biogeochem. Cy.* 27 (3): 723–31. doi:10.1002/gbc.20061.

Matrai, P., and S. Apollonio. 2013. "New estimates of microalgae production based upon nitrate reductions under sea ice in Canadian shelf seas and the Canada Basin of the Arctic Ocean." *Mar. Biol.* 160: 1297–1309. doi:10.1007/s00227-013-2181-0.

McCabe, G.J., M.P. Clark, and M.C. Serreze. 2001. "Trends in Northern Hemisphere surface cyclone frequency and intensity." *J. Clim.* 14: 2763−2768.

Mei, Z.-P., L. Legendre, Y. Gratton, J.-É. Tremblay, B. LeBlanc, C.J. Mundy, B. Klein, M. Gosselin, C. Larouche, P. Papakyriakou, T.N. Lovejoy, and C.H. von Quillfeldt. 2002. "Physical control of spring–summer phytoplankton dynamics in the North Water, April–July 1998." *Deep-Sea Res. Pt II* 49: 4959–82.

Michel, C., J. Hamilton, E. Hansen, D. Barber, M. Reigstad, J. Iacozza, L. Seuthe, and A. Niemi. 2015. "Arctic Ocean outflow shelves in the changing Arctic: A review and perspectives." *Prog. Phys. Geog.* doi:10.1016/j.pocean.2015.08.007.

Michel, C., K.A. Hobson, M. Gosselin, and N.M. Price. 2006. "Bloom dynamics in early opening waters of the Arctic Ocean." *Prog. Ocean.* 51 (2): 900–912.

Mueller, D., A. Crawford, L. Copland, and W. Van Wychen. 2013. "'Ice Island and Iceberg Fluxes from Canadian High Arctic Sources." Report Prepared for the Northern Transportation Assessment Initiative, Innovation Policy Branch, Transport Canada. Ottawa, Ontario, pp 23.

Mueller, D.R., W.F. Vincent, and M.O. Jeffries. 2003. "Break-up of the largest Arctic ice shelf and associated loss of an epishelf lake." *Geophys. Res. Lett* 30 (20): 2031. doi:10.1029/2003GL017931.

Mueller, D.R., W.F. Vincent, and M.O. Jeffries. 2006. "Environmental gradients, fragmented habitats, and microbiota of a northern ice shelf cryoecosystem, Ellesmere Island , Canada." *Arct. Ant. Alp. Res.* 38 (4): 593–607.

Mueller, D.R., L. Copland, A. Hamilton, and D. Stern. 2008. "Examining Arctic ice

shelves prior to the 2008 breakup." *EOS* 89 (49): 502–3.

Mundy, C.J., M. Gosselin, J. Ehn, Y. Gratton, A. Rossnagel, M. Palmer, D.G. Barber, J. Martin, J- É Tremblay, M. Palmer, K.R. Arrigo, G. Darnis, L. Fortier, B. Else, and T. Papakyriakou. 2009. "Contribution of under-ice primary production to an ice-edge upwelling phytoplankton bloom in the Canadian Beaufort Sea." *Geophys. Res. Lett.* 36: 1–5. doi:10.1029/2009GL038837.

Mundy, C.J., M. Gosselin, Y. Gratton, K. Brown, V. Galindo, K. Campbell, M. Levasseur, D. Barber, T. Papakyriakou, and S. Belanger. 2014. "Role of environmental factors on phytoplankton bloom initiation under landfast sea ice in Resolute Passage, Canada." *Mar. Ecol. Prog. Ser.* 497: 39–49.

Neshyba, S. 1977. "Upwelling by icebergs." *Nature* 267: 507–8.

Newell, J.P. 1993. "Exceptionally large icebergs and ice islands in eastern Canadian Waters: A review of sightings from 1900 to present." *Arctic* 46: 205–11.

Overland, J. E., J. A. Francis, E. Hanna, and M. Wang. 2012. "The recent shift in early summer Arctic atmospheric circulation." *Geophys. Res. Lett.* 39: L19804. doi:10.29/2011GL047735.

Parsons, T.R., Y. Maita, and C. Lalli. 1984. A Manual of Chemical and Biological Methods for Seawater Analysis, Pergamon Press, Toronto. pp. 184.

Peterson, I.K. 2005. "Large tabular icebergs and ice islands off eastern Canada in 2001-2003 and their probable source." Proc., 18th Int. Conf. on Port and Ocean Eng. Under Arctic Conditions. 1:143-152.

Platt, T., W.G. Harrison, E.P.W. Horne, and B. Irwin. 1987. "Carbon fixation and oxygen evolution by phytoplankton in the Canadian High Arctic." *Polar Biol.* 8:103–13.

Price, J.F., R.A. Weller, and R.R. Schudlich. 1987. "Wind-driven ocean currents and Ekman transport." *Science* 238 (4833): 1534–38.

Redfield, A.C., B. Ketchum, and F. Richards. 1963. "The influence of organisms on the composition of sea-water." In: Hill, M. (Eds.), The Sea. New York, US: Interscience. pp. 26-77.

Reigstad, M., P. Wassmann, C. W. Riser, S. Øygarden, and F. Rey. 2002. "Variations in hydrography, nutrients and chlorophyll *a* in the marginal ice-zone and the central Barents Sea." *J. Marine Syst.* 38 (1): 9–29.

Reynolds, C.S., 2006. The Ecology of Phytoplankton. 1st ed. Cambridge University Press, New York. pp. 535.

Rignot, E., and K. Steffen. 2008. "Channelized bottom melting and stability of floating ice shelves." *Geophys. Res. Lett.* 35: L02503. doi:10.1029/2007GL031765.

Robinson, N.J., M.J.M. Williams, P.J. Barrett, and A.R. Pyne. 2010. "Observations of flow and ice-ocean interaction beneath the McMurdo Ice Shelf, Antarctica." *J. Geophys. Res.* 115: C03025. doi:10.1029/2008JC005255.

Rozanska, M., M. Gosselin, M. Poulin, J. M. Wiktor, and C. Michel. 2009. "Influence of environmental factors on the development of bottom ice protist communities during the winter- spring transition." *Mar. Ecol. Prog. Ser.* 386: 43–59. doi:10.3354/meps08092.

Rudels, B., A-M. Larsson, and P.I. Sehlstedt. 1991. "Stratification and water mass formation in the Arctic Ocean: Some implications for the nutrient distribution." *Polar Res.* 10 (1).

Rudkin, P., T. King, F. Ralph, and S.A. Stoermer. 2005. "Investigations into the increased sightings of ice islands in the North Atlantic". Proceedings of the 18th International Conference on Port and Ocean Engineering Under Arctic Conditions Held 26-30 June in Potsdam, NY. 2:605–14.

Sakshaug, E. 2004. "Primary and secondary production in the Arctic Seas." In: Stein, R., Macdonald, R.W. The Organic Carbon Cycle in the Arctic Ocean. Springer, Berlin, Heidelberg.

Redfield, A.C., B. Ketchum, and F. Richards. 1963. "The influence of organisms on the composition of sea-water." In: Hill, M. (Eds.), The Sea. New York, US: Interscience. pp. 26-77.

Savage, S.B. 2001. "Aspects of iceberg deterioration and drift." In: N.J. Balmforth and A. Provenzale (Eds.), Geomorphological Fluid Mechanics. LNP 582. Springer-Verlag. Berlin, Heidelberg. pp. 279–318.

Schlitzer, R. 2015. "Ocean Data View." http://odv.awi.de.

Schwarz, J.N., and M.P. Schodlok. 2009. "Impact of drifting icebergs on surface phytoplankton biomass in the Southern Ocean: Ocean colour remote sensing and *in situ* iceberg tracking." *Deep-Sea Res. Pt I* 56: 1727–41. doi:10.1016/j.dsr.2009.05.003.

Send, U., R. C. Beardsley, and C. D. Winant. 1987. "Relaxation from upwelling in the coastal ocean dynamics experiment." *J. Geophys. Res.* 92: 1683–98.

Serreze, M.C., and R.G. Barry. 2011. "Processes and impacts of Arctic amplification: A Research synthesis." *Global Planet. Change* 77 (1-2): 85–96. doi:10.1016/j.gloplacha.2011.03.004.

Siegenthaler, U., and J.L. Sarmiento. 1993. "Atmospheric carbon dioxide and the ocean." *Nature* 365 (6442): 119–25.

Simpson, K., J. Martin, L. Miller, Y. Gratton, D. Barber, and N.M. Price. 2008. "Vertical

stability and the annual dynamics of nutrients and chlorophyll fluorescence in the coastal, Southeast Beaufort Sea" 113: 1–14. doi:10.1029/2007JC004547.

Smith, K.L., B.H. Robison, J.J. Helly, R.S. Kaufmann, H.A. Ruhl, T.J. Shaw, B.S. Twining, and M. Vernet. 2007. "Free-drifting icebergs: Hot spots of chemical and biological enrichment in the Weddell Sea." *Science* 317, 478-482. doi:10.1126/science.1142834.

Steinacher, M., F. Joos, T.L. Frolicher, L. Bopp, P. Cadule, V. Cocco, S.C. Doney, M. Gehlen, K. Lindsay, J. Moore, K.B. Schneider, J. Segschneider. 2010. "Projected 21st century decrease in marine productivity: A multi-model analysis." *Biogeosciences* 7: 979–1005.

Stephenson, G.R., J. Sprintall, S.T. Gille, M. Vernet, J.J. Helly, and R.S. Kaufmann. 2011. "Subsurface melting of a free-floating Antarctic iceberg." *Deep-Sea Res. Pt II* 58: 1336–45. doi:10.1016/j.dsr2.2010.11.009.

Stern, A.A., E. Johnson, D.M. Holland, T.J.W. Wagner, P. Wadhams, R. Bates, E.P. Abrahamsen, K.W. Nicholls, A. Crawford, J. Gagnon, and J.-É. Tremblay. 2015. "Wind-driven upwelling around grounded tabular icebergs." *J. Geophys. Res. Oceans*. doi:10.1002/2015JC010805.

Sterner, R.W., T. Andersen, J. J. Elser, D. O. Hessen, J. M. Hood, E. McCauley, and J. Urabe. 2008. "Scale-dependent carbon:nitrogen:phosphorus seston stoichiometry in marine and freshwaters." *Limnol. Oceanogr.* 53 (3): 1169–80. doi:10.4319/lo.2008.53.3.1169.

Taucher, J., and A. Oschlies. 2011. "Can we predict the direction of marine primary production change under global warming?" *Geophys. Res. Lett.* 38: 1–6. doi:10.1029/2010GL045934.

Tremblay, G., C. Belzile, M. Gosselin, M. Poulin, S. Roy, and J.-É. Tremblay. 2009. "Late summer phytoplankton distribution along a 3500 km transect in Canadian Arctic waters: Strong numerical dominance by picoeukaryotes." *Aquat. Microb. Ecol.* 54: 55–70.

Tremblay, J.-É., S. Bélanger, D.G. Barber, M. Asplin, J. Martin, G. Darnis, L. Fortier, Y. Gratton, H. Link, P. Archambault, A. Sallon, C. Michel, W.J. Williams, B. Philippe, and M. Gosselin. 2011. "Climate forcing multiplies biological productivity in the coastal Arctic Ocean." *Geophys. Res. Lett.* 38: 2–6. doi:10.1029/2011GL048825.

Tremblay, J.-É., and J. Gagnon. 2009. "The Effects of irradiance and nutrient supply on the productivity of Arctic waters: A perspective on climate change." In: J.C.J. Nihouland and A. Kostianoy (Eds.), Influence of Climate Change in the Changing Arctic and Sub-Arctic Conditions. Springer, Dordrecht. pp. 73–94.

Tremblay, J.-É. K. Simpson, J. Martin, L. Miller, Y. Gratton, D. Barber, and N.M. Price. 2008. "Vertical stability and the annual dynamics of nutrients and chlorophyll

fluorescence in the coastal, southeast Beaufort Sea." *J. Geophys. Res.* 113: 7–90. doi:10.1029/2007JC004547.

Tremblay, J.-É., Y. Gratton, J. Fauchot, and N.M. Price. 2002. "Climatic and oceanic forcing of new, net, and diatom production in the North Water." *Deep-Sea Res. Pt II* 49: 4927–46.

Tremblay, J.-É, C. Michel, K.A. Hobson, and M. Gosselin. 2006. "Bloom dynamics in early opening waters of the Arctic Ocean." *Limnol. Oceanogr.* 51 (2): 900–912.

Tung, H.C., P.B. Price, N.E. Bramall, and G. Vrdoljak. 2006. "Microorganisms metabolizing on clay grains in 3-km-deep Greenland basal ice." *Astrobiology* 6: 69–86.

Vernet, M., K. Sines, D. Chakos, A.O. Cefarelli, and L. Ekern. 2011. "Impacts on phytoplankton dynamics by free-drifting icebergs in the NW Weddell Sea." *Deep-Sea Res. Pt II* 58 (11-12): 1422–35. doi:10.1016/j.dsr2.2010.11.022.

Walsh, J.J., D. A. Dieterle, W. Maslowski, and T. E. Whitledge. 2004. "Decadal shifts in biophysical forcing of Arctic marine food webs: Numerical consequences." *J. Geophys. Res.* 109: C05031. doi:10.1029/ 2003JC001945.

Wassmann, P., and M. Reigstad. 2011. "Future Arctic Ocean seasonal ice zones and implications for pelagic-benthic coupling." *Oceanography* 24 (3): 220–31.

Welch, H., and M.A. Bergmann. 1989. "Seasonal development of ice algae and its prediction from environmental factors near Resolute, N.W.T., Canada." *Can. J. Fish. Aquat. Sci.* 46: 1793–1804.

Williams, W.J. and E.C. Carmack. 2015. "The interior shelves of the Arctic Ocean: Physical oceanographic setting, climatology and effects of sea-ice retreat on cross-shelf exchange." *Prog. Oceanogr*. 139: 24-41.

WMO. 1970. "'Sea-Ice Nomenclature' World Meteorological Organization." Geneva, Report 259.

Yamamoto-Kawai, M., E.C. Carmack, F.A. McLaughlin, and K.K. Falkner. 2010. "Oxygen isotope ratio, barium and salinity in waters around the North American coast from the Pacific to the Atlantic: Implications for freshwater sources to the Arctic throughflow." *J. Mar. Res.* 68: 97–117.

Yamamoto-Kawai, M., F.A. McLaughlin, E.C. Carmack, S. Nishino, K. Shimada, and N. Kurita. 2009. "Surface freshening of the Canada Basin, 2003−2007: River runoff versus sea ice meltwater." *J. Geophys. Res.* 114: C00A05. doi:10.1029/ 2008JC005000.

Yang, J. 2009. "Seasonal and interannual variability of downwelling in the Beaufort Sea." *J. Geophys. Res.* 114: C00A14. doi:10.1029/2008JC005084.

Zhang, X., J.E. Walsh, J. Zhang, U.S. Bhatt, and M. Ikeda. 2004. “Climatology and interannual variability of Arctic cyclone activity: 1948−2002.” *J. Clim.* 17: 2300−2317.

## Appendices

**Appendix A** Station numbers for profiling (CTD and C3) and water sampling on each sampling day (dd/mm/yyyy). Analyses include salinity, $\delta^{18}O$, nutrients, dissolved organic carbon (DOC), protist counts by flow cytometry (FCM), and total and >5 µm chlorophyll *a* (Chl*a*) at the surface and 4 depths (5, 10, 25 and 50).

| Date | Transect | Profile | | Variables | | | | | | | |
|---|---|---|---|---|---|---|---|---|---|---|---|
| | | | | Surface | | | | Depths (5, 10, 25, 50 m) | | | |
| | | CTD | C3 | Salinity, nutrients, $\delta^{18}O$ | DOC | FCM | Chl*a* tot and Chl*a* >5um | Salinity, nutrients, $\delta^{18}O$ | DOC | FCM | Chl*a* tot and Chl*a* >5um |
| 11/08/2014 | N | 1 | 1, 4 | 1 | | | | | | | |
| | S | 1, 2, 3, 5, 7 | | 1, 2, 3, 5, 7 | | | | | | | |
| | E | 1, 2, 3,4 | | 1, 2, 3,4 | | | | | | | |
| | W | 1, 2, 3, 4, 5 | | 1, 2, 3, 4, 5 | | | | | | | |
| | A or B | B01 | | | | | | | | | |
| 16/08/2014 | W | 1 | 1 | 1 | 1 | 1 | 1 | 1 | 1 | 1 | 1 |
| | A or B | | B01 | B01 | B01 | B01 | B01 | B01, A01* | B01, A01* | B01, A01* | B01, A01* |
| 25/08/2014 | N | | | | | | | | | | |
| | S | 4, 5, 6, 7, 8, 9, 10, 11 | 11 | 11 | 11 | 11 | 11 | 11 | 11 | 11 | 11 |

| | | | | | | | | | | | |
|---|---|---|---|---|---|---|---|---|---|---|---|
| | W | 1 | 1 | 1 | 1 | 1 | 1 | 1 | 1 | 1 | 1 |
| 28/08/2014 | N | 2 | | | | | | | | | |
| | S | 2, 4, 5, 7, 11 | 11 | | | | | 11** | 11** | 11** | |
| | E | | | | | | | | | | |
| | W | 1 | 1 | 1 | 1 | 1 | 1 | 1 | 1 | 1 | 1 |
| 29/08/2014 | N | | | | | | | | | | |
| | S | 1, 4, 5, 7 | 1, 4, 5, 7 | 1, 4, 5, 7 | 1, 4, 5, 7 | 1, 4, 5, 7 | 1, 4, 5, 7 | | | | |
| | E | 2, 3 | 2, 3 | 2, 3 | 2, 3 | 2, 3 | 2, 3 | | | | |
| | W | 1 | 1 | 1 | 1 | 1 | 1 | | | | |

*Samples were only taken at 80 m depth.

** Samples were only taken at 110 m depth